A&A 507, 1117–1139 (2009)
DOI: 10.1051/0004-6361/200912135

Astronomy & Astrophysics

Absolute positions of 6.7-GHz methanol masers

Y. Xu[1,2], M. A. Voronkov[3,4], J. D. Pandian[1], J. J. Li[5], A. M. Sobolev[6], A. Brunthaler[1], B. Ritter[1], and K. M. Menten[1]

[1] Max-Planck-Institute für Radioastronomie, Auf dem Hägel 69, 53121 Bonn, Germany
[2] Purple Mountain Observatory, Chinese Academy of Sciences, Nanjing 210008, PR China
e-mail: xuye@pmo.ac.cn
[3] Australia Telescope National Facility CSIRO, PO Box 76, Epping, NSW 1710, Australia
[4] Astro Space Centre, Profsouznaya st. 84/32, 117997 Moscow, Russia
[5] Key Laboratory for Research in Galaxies and Cosmology, Shanghai Astronomical Observatory, Chinese Academy of Sciences, Shanghai, 20030, PR China
[6] Ural State University, Ekaterinburg, 620083, Russia

Received 23 March 2009 / Accepted 24 July 2009

ABSTRACT

The ATCA, MERLIN and VLA interferometers were used to measure the absolute positions of 35 6.7-GHz methanol masers to subarcsecond or higher accuracy. Our measurements represent essential preparatory data for Very Long Baseline Interferometry, which can provide accurate parallax and proper motion determinations of the star-forming regions harboring the masers. Our data also allow associations to be established with infrared sources at different wavelengths. Our findings support the view that the 6.7 GHz masers are associated with the earliest phases of high-mass star formation.

Key words. masers – instrumentation: interferometers – astrometry – Galaxy: structure

1. Introduction

The 5_1-6_0 A^+ transition of methanol at 6.7-GHz produces the brightest methanol masers (Menten 1991). The masers are widespread in the Galaxy and more than 550 sources have been detected to date, including the compilations of Xu et al. (2003), Malyshev & Sobolev (2003), and Pestalozzi et al. (2005), and the searches of Caswell et al. (1995a), Caswell (1996a, 1996b), MacLeod et al. (1998), Szymczak et al. (2000), Pandian et al. (2007), Ellingsen (2007), and Xu et al. (2008).

It has been shown that 12.2-GHz methanol masers are excellent tools for determining the distances to massive star-forming regions by measuring their trigonometric parallax using very long baseline interferometry (VLBI) (e.g., Xu et al. 2006a). The 2_0-3_{-1} E transition at 12.2-GHz is the second brightest methanol maser transition and the locations of the 6.7-GHz and 12.2-GHz methanol maser spots largely overlap, with several features showing a one-to-one correspondence within milliarcseconds and the spectra of the two transitions typically covering similar velocity ranges (Menten et al. 1992; Norris et al. 1993; Minier et al. 2000). Since 6.7 GHz masers are almost always stronger, i.e., *much* stronger than their 12.2-GHz counterparts, they are also expected to be a useful for probing distances to massive star-forming regions in the Galaxy. Measuring accurate distances are critical for studying the massive star-forming regions individually and understanding the distribution of these regions in the context of our perception of the Galaxy's spiral structure.

For phase-referenced VLBI observations (mandatory for high precision astrometry), one usually employs strong masers as the phase-reference, and synthesizes images of nearby extragalactic continuum sources. The astrometric precision scales with the source separation and, statistically, weaker sources are found closer to masers. These sources can be detected (e.g., by VLA observations; see Xu et al. 2006b). On the other hand, for a successful VLBI astrometric measurement, one requires a position estimate of the maser position that is accurate to at least 1″, as input in the correlator. This means that a large number of masers in the literature have positions determined with single dish observations that are not accurate enough for VLBI observations. Here we report absolute position measurements of 35 6.7-GHz methanol masers with subarcsecond accuracy using the Australia Telescope Compact Array (ATCA), MERLIN and the NRAO Very Large Array (VLA). Most of the sources in our study are associated with 12.2-GHz counterparts.

2. Observations and data reduction

The ATCA observations were completed in 2006 April in the 6C configuration, which produces baselines from 153 to 6000 m. The observations were done in snap-shot mode. Each source was observed in six 5-min scans spread over a range of hour angles to ensure a good uv-coverage. The correlator was configured to have a 4 MHz bandwidth with 1024 spectral channels. Two orthogonal linear polarizations were observed and averaged together during the data processing. The full width at half-maximum ($FWHM$) of the primary beam was 7.2′. The default pointing model was used, giving an rms pointing accuracy of around of 5–10″. The accuracy of the pointing model affects the accuracy of the flux density measurements, particularly for sources that are offset from the pointing center. The absolute flux density scale was determined from observations of PKS B1934–638. The accuracy of the flux density calibration is expected to

be approximately 3%[1]. The bandpass calibration was carried out using observations of the continuum source 1921–293. The data were reduced with the MIRIAD package using standard procedures.

The MERLIN observations were carried out in 2007 February using six telescopes, and in 2007 March using five telescopes. The correlator was used in two modes. The phase reference sources and the primary calibrator (3C84) were observed in wide-band mode with a bandwidth of 16 MHz and 32 spectral channels. The bandpass calibrator (also 3C84) and the targets were observed in the narrow-band mode with 2 MHz bandwidth and 256 spectral channels. The total on-source integration time per source was over 1 h, divided into a number of 5 min scans to achieve good uv-coverage. The flux density of 3C84 was assumed to be 14.5 Jy in February 2007 and 15 Jy in March 2007. The initial calibration and conversion of the data to FITS format was done using the local MERLIN software, and subsequent analysis was done using the Astronomical Image Processing System (AIPS). The instrumental phase offset between the wide band and narrow band data was derived using 3C84 (see the MERLIN User Guide for details; Diamond et al. 2003).

The VLA observations were conducted on 2009 January 27 in BnA configuration using 18 EVLA antennas. The observations were done in single IF mode (A1, RCP) with each source being observed in three scans with an integration time of 2.75 min per scan. The full 3.125 MHz bandwidth was divided into 256 channels. For all target sources the bandwidth was always centered on the velocity of 14.75 km s^{-1} with respect to the local standard of rest. The primary beam was 6.75′. The total flux density of the flux calibrator 3C 286 was calculated to be 6.072 Jy. The source 2007+404 served as a bandpass calibrator and 2084+431 was the phase reference calibrator for all target sources.

The spectral resolution was 0.18, 0.35 and 0.55 km s^{-1} for the ATCA, MERLIN and VLA observations, respectively. The rest frequency of 6668.5192 MHz was assumed for all observations.

After imaging the targets, the AIPS package task "JMFIT" was used to determine the fluxes and positions of each maser feature in all observations.

3. Results

The accuracy of the absolute maser positions is limited by several factors, such as source elevation, weather conditions, length and type of observations, position accuracy of the phase calibrator, and signal-to-noise ratio. For the ATCA data, the typical signal-to-noise ratio is over 500, and the phase calibrators have positions accurate to better than 0.15″. Hence, we assume that most of the target sources have an absolute position accuracy of 0.5″ or higher, except for sources that are close to the celestial equator. This is a typical position accuracy of ATCA data (Caswell et al. 1995c; Walsh et al. 1998; Phillips et al. 1998; Minier et al. 2001; Caswell 2009). For the MERLIN data, the typical signal-to-noise ratio is at least 100, and all but one phase calibrator are from the Jodrell Bank–VLA Astrometric Survey, which has a position accuracy of higher than 5 ms. Hence, we estimate that the absolute positions of the target sources are accurate to within 0.1″. The source *IRAS* 20290+4052 was observed by both the VLA and MERLIN, and the VLA positions deviate from the MERLIN positions by 0.05″. On the other hand, our previous observations with the VLA B configuration have a position uncertainty of better than 0.1″ (Xu et al. 2006b). Therefore, a position uncertainty of better than 0.1″ is expected for sources observed with the VLA. A position uncertainty of better than 1″ is sufficient for successful observations using the European VLBI Network (EVN) and the Very Long Baseline Array (VLBA), for example to determine parallax measurements.

Tables 1–3 list the properties of the 6.7-GHz methanol sources observed with the ATCA, MERLIN, and VLA, respectively. For sources that exhibit multiple masing spots, the properties of individual spots are given in separate rows. In the three tables, the first three columns show the source name and J2000 equatorial coordinates. Columns 4 and 5 give their Galactic coordinates. Columns 6 and 7 show the radial velocity of the maser peak and that of the molecular lines, respectively. Column 8 presents the peak flux density. Columns 9 to 11 present the distance of the source from the Galactic center and its heliocentric kinematical distance. The kinematical distances were calculated using the velocities of molecular lines, such as CO, CS, and NH_3 (where these data are available; for other sources, the maser peak velocity was used) and the Galactic rotation model of Wouterloot & Brand (1989), assuming $R_0 = 8.5$ kpc and $\Theta_0 = 220$ km s^{-1}. The uncertainties in kinematic distances were estimated by applying ±10 km s^{-1} velocity offsets.

3.1. Notes on selected sources

The spectra of the 6.7-GHz methanol masers are shown in Figs. 3–5, for sources observed with the ATCA, MERLIN, and VLA, respectively . The ATCA data have a velocity resolution of 0.18 km s^{-1} which is sufficient to resolve the multiple velocity components of each source. The velocity resolution of the VLA data is 0.55 km s^{-1}. The velocity resolution of the MERLIN data is only 0.7 km s^{-1} after Hanning smoothing (because of the limitations of the correlator), which results in the blending of individual components in the spectra. Here we present notes on some sources.

G8.8316–0.0281 . There are at least six features within the velocity range of 10 km s^{-1} that have peak flux densities exceeding 10 Jy/beam. The strongest feature is at the LSR velocity of −3.9 km s^{-1}.

G8.8722–0.4928. There are only two features stronger than 10 Jy/beam, at +23.4 and +24.1 km s^{-1}. The two features are spectrally blended together.

G14.1014+0.0869. There are a number of features located within a 0.2″ × 0.2″ region. The strongest 6.7 GHz peak is at the velocity of the second strongest 12.2-GHz feature (Blaszkiewicz & Kus 2004).

G23.0099–0.4107. The features span the velocity range from 70.1 to 83.2 km s^{-1}, as do the 12.2-GHz maser features in this source, although they do not coincide precisely. There are at least 5 features for which the peak flux density exceeds 10 Jy/beam. The strongest feature is at the same velocity as the strongest 12.2-GHz maser (Caswell et al. 1995b). However, the 6.7-GHz feature corresponding to the second strongest 12.2-GHz feature at +76.6 km s^{-1} is not clearly distinguishable from the other lines.

G23.2068–0.3777. This source has two prominent peaks. The strongest feature is at the same velocity, 81.7 km s^{-1}, as the strongest feature at 12.2-GHz (Blaszkiewicz & Kus 2004).

[1] For details of the calibration using 1934–638, query this calibrator at the ATCA calibrators webpage (http://www.narrabri.atnf.csiro.au/calibrators).

Table 1. 6.7-GHz methanol masers observed with ATCA.

Source name	RA(2000) ($^h\,^m\,^s$)	Dec(2000) ($^\circ\,'\,''$)	l ($^\circ$)	b ($^\circ$)	V_{LSR} (km s^{-1})	V_{mol} (km s^{-1})	S_{peak} (Jy/beam)	R (kpc)	d_{far} (kpc)	d_{near} (kpc)
*G*8.832-0.028	18 05 25.66	–21 19 25.5	8.832	–0.028	–3.9	0.5(1)	132.0	8.4	16.7(±3.6)	0.1(±2.0)
*G*8.872-0.493	18 07 15.32	–21 30 54.4	8.872	–0.493	23.4		30.9	4.9	13.2(±1.1)	3.6(±1.1)
*G*14.101+0.087	18 15 45.80	–16 39 09.7	14.101	0.087	15.2	9.3(2)	90.2	7.2	15.1(±1.5)	1.3(±1.1)
	18 15 45.80	–16 39 09.5	14.101	0.087	5.9		15.4			
	18 15 45.81	–16 39 09.5	14.102	0.087	10.1		25.1			
	18 15 45.81	–16 39 09.6	14.101	0.087	11.0		22.8			
	18 15 45.80	–16 39 09.7	14.101	0.087	13.1		16.3			
	18 15 45.80	–16 39 09.7	14.101	0.087	13.6		22.6			
*G*23.010-0.411	18 34 40.29	–09 00 38.1	23.010	–0.411	74.8	74.8(2)	415.4	4.4	10.8(±0.5)	4.9(±0.5)
	18 34 40.29	–09 00 38.2	23.010	–0.411	72.7		43.4			
	18 34 40.28	–09 00 38.4	23.010	–0.411	80.6		49.1			
	18 34 40.28	–09 00 38.4	23.010	–0.411	81.6		52.0			
	18 34 40.27	–09 00 38.5	23.010	-0.411	82.3		43.4			
*G*23.207-0.378	18 34 55.20	–08 49 14.2	23.207	–0.378	81.7		38.2	4.3	10.5(±0.5)	5.2(±0.5)
	18 34 55.21	–08 49 14.4	23.207	–0.378	76.5		19.4			
	18 34 55.21	–08 49 14.6	23.207	–0.378	77.0		35.4			
*G*24.148-0.009	18 35 20.94	–07 48 55.6	24.148	–0.009	17.7	23.1(3)	26.8	6.7	13.5(±0.8)	2.0(±0.8)
*G*24.329+0.144	18 35 08.14	-07 35 04.0	24.329	0.144	110.2	112.0(2)	5.0	3.7	8.9(±0.9)	6.6(±0.9)
*G*27.220+0.260	18 40 03.72	–04 57 45.6	27.220	0.260	9.3		6.2	7.8	14.3(±0.9)	0.8(±0.8)
*G*27.365-0.166	18 41 51.06	–05 01 42.8	27.365	–0.166	100.0	92.2(4)	28.0	4.2	9.2(±0.7)	5.9(±0.7)
	18 41 51.06	–05 01 42.8	27.365	–0.166	98.0		10.2			
	18 41 51.06	–05 01 42.8	27.365	–0.166	98.9		13.7			
	18 41 51.06	–05 01 42.8	27.365	–0.166	100.7		14.2			
	18 41 51.06	–05 01 42.7	27.365	–0.166	101.5		10.8			
*G*29.863-0.044	18 45 59.57	–02 45 04.4	29.863	–0.044	101.4	100.4(4)	76.5	4.3	8.2(±0.8)	6.6(±0.8)
	18 45 59.57	–02 45 04.5	29.863	–0.044	100.3		52.0			
	18 45 59.57	–02 45 04.5	29.863	–0.044	101.7		54.2			
*G*30.199-0.169	18 47 03.07	–02 30 33.6	30.199	–0.169	108.6	103.3(4)	16.0	4.3	7.8(±1.0)	6.9(±1.0)
*G*30.225-0.180	18 47 08.30	–02 29 27.1	30.225	–0.180	113.5	104.5(4)	10.8	4.3	7.7(±1.1)	7.0(±1.1)
*G*30.899+0.162	18 47 09.13	–01 44 08.8	30.899	0.162	101.8		25.7	4.4	7.7(±1.1)	6.9(±1.1)
	18 47 09.13	–01 44 08.7	30.899	0.162	103.0		14.2			

The first column lists the source name. The next two columns give their J2000 equatorial coordinates. Columns (4) and (5) give their galactic coordinates. Columns (6) and (7) show the radial velocity of peak emission from the maser and molecular lines. Column (8) presents the peak flux density. Columns (9)–(11) present the distance from the Galactic center, and the far and near kinematic distances.
References for the velocities: 1 – Zhang et al. (2005); 2 – Larionov et al. (1999); 3 – Szymczak et al. (2007); 4 – van der Walt et al. (2007).

G24.1480–0.0092. The spectra at both 6.7-GHz and 12.2-GHz (Blaszkiewicz & Kus 2004) are similar and dominated by a single feature.

G27.3652–0.1659. There are clearly five features with peak flux densities exceeding 10 Jy/beam. The emission has a spatial extent of 0.1″ and is confined to a narrow velocity range of approximately 5 km s^{-1}. The 12.2-GHz spectrum is dominated by a single feature (Caswell et al. 1995b). The peak velocity is the same for both 6.7 and 12.2-GHz masers. Our observations detected an unresolved 8.6 GHz continuum source that is offset by about 2.4″ from the maser.

G29.8630–0.0442. There are three strong features within an area of 0.1″ × 0.1″. The strongest feature at 6.7-GHz matches the velocity of the second strongest 12.2-GHz feature and vice versa (Caswell et al. 1995b).

G30.1987–0.1687 and **G30.2251-0.1796**. The two sources are separated by 103″. The peak velocities are +108.6 km s^{-1} and +113.5 km s^{-1} for G30.1987–0.1687 and G30.2251–0.1796, respectively. There are two corresponding 12.2-GHz features at +108.5 and +110.2 km s^{-1}, respectively (Caswell et al. 1995b), which are likely to originate in the same two emission centres. However, a high angular resolution study at 12.2-GHz is required to confirm this. Although there are a number of features in both sources, only these two peaks have peak flux densities that exceed 10 Jy/beam.

G30.8987+0.1616. There are two features with peak flux densities exceeding 10 Jy/beam. The emission peaks at 12.2 and 6.7 GHz are close in velocity.

S255. The spectrum of Szymczak et al. (2000) shows multiple spectral features, which are not visible in the VLA spectrum because of its poor velocity resolution. However, imaging shows two maser sites separated by 0.2″.

18556+0136. The spectrum of Szymczak et al. (2000) shows multiple spectral features. However, in this study we found only a single feature. The 12.2-GHz spectrum also has multiple features, but is dominated by just two peaks (Caswell et al. 1995b).

G43.15+0.02. The spectrum of Caswell et al. (1995a) indicated that multiple features were present. We detected only one spectral feature. Its velocity corresponds to that of the strongest 12.2 GHz feature (Caswell et al. 1995b).

Table 2. Same as Table 1 for the 6.7-GHz methanol masers observed with MERLIN.

Source name	RA(2000) ($^h\,^m\,^s$)	Dec(2000) ($^\circ\,'\,''$)	l ($^\circ$)	b ($^\circ$)	$V_{\rm LSR}$ (km s^{-1})	$V_{\rm mol}$ (km s^{-1})	$S_{\rm peak}$ (Jy/beam)	R (kpc)	$d_{\rm far}$ (kpc)	$d_{\rm near}$ (kpc)
*L*1287	00 36 47.358	63 29 02.18	121.298	0.659	–23.2	–17.6(3)	7.5	9.4	1.6(±0.9)	
*NGC*281 – *N*	00 52 24.196	56 33 43.17	123.066	–6.309	–29.3	–31.8(3)	32.4	10.4	2.9(±1.0)	
*S*231	05 39 13.066	35 45 51.29	173.482	2.446	–12.8	–15.8(3)	32.1	24.1	15.6(±12.9)	
*AFGL*5180	06 08 53.342	21 38 29.09	188.946	0.886	10.7	3.1(1)	194	9.4	0.9(±4.7)	
*AFGL*6366	06 08 40.671	21 31 06.89	189.030	0.784	8.8	2.5(1)	1.6	9.2	0.7(±4.4)	
*S*255	06 12 54.006	17 59 23.21	192.600	–0.048	5.5	8.2(3)	10.0	10.3	1.9(±3.6)	
	06 12 54.020	17 59 23.27	192.600	–0.048	4.4		8.5			
*S*269	06 14 37.051	13 49 36.16	196.454	–1.677	15.3	17.9(1)	3.6	12.1	3.7(±3.7)	
18556+0136	18 58 13.053	01 40 35.68	35.197	–0.743	28.5	35.0(3)	72.8	6.6	11.4(±0.6)	2.5(±0.6)
*G*43.15 + 0.02	19 10 11.049	09 05 20.49	43.149	0.013	13.4	2.9(1)	6.0	8.3	12.2(±0.8)	0.2(±0.8)
19120+0917	19 14 26.393	09 22 36.53	43.890	–0.784	52.0	54.2(1)	3.0	6.2	8.1(±1.6)	4.2(±1.6)
	19 14 26.392	09 22 36.62	43.890	–0.784	47.7		4.5			
19186+1440	19 20 59.212	14 46 49.65	49.416	0.326	–12.1		7.0	9.2	12.1(±0.9)	
W51e2	19 23 43.949	14 30 34.44	49.490	–0.388	59.2	56.5(3)	217			
19303+1651	19 32 36.071	16 57 38.46	52.663	–1.092	65.7	59.7(1)	1.3			
*ON*1*A*	20 10 09.047	31 31 35.06	69.540	–0.976	14.7	11.7(3)	31.0	8.0	4.0(±1.7)	2.0(±1.8)
*ON*1*B*	20 10 09.073	31 31 35.94	69.540	–0.976	–0.1	11.7(3)	8.8	8.0	4.0(±1.7)	2.0(±1.8)
20290+4052	20 30 50.673	41 02 27.55	79.736	0.991	–5.2	–1.4(1)	18.2	8.6	3.3(±1.5)	
21381+5000	21 39 58.263	50 14 20.96	94.602	–1.796	–40.7	–45.6(3)	4.2	10.8	6.1(±1.1)	
	21 39 58.262	50 14 21.05	94.603	–1.796	–43.6		4.0			
*L*1206	22 28 51.408	64 13 41.30	108.184	5.519	–11.0	–9.9(2)	29.4	8.9	1.2(±1.1)	

References for the velocities: 1 – Bronfman et al. (1996); 2 – Molinari et al. (1996); 3 – Plume et al. (1992).

Table 3. Same as Table 1 for the 6.7-GHz methanol masers observed with VLA.

Source name	RA(2000) ($^h\,^m\,^s$)	Dec(2000) ($^\circ\,'\,''$)	l ($^\circ$)	b ($^\circ$)	$V_{\rm LSR}$ (km s^{-1})	$V_{\rm mol}$ (km s^{-1})	$S_{\rm peak}$ (Jy/beam)	R (kpc)	$d_{\rm far}$ (kpc)	$d_{\rm near}$ (kpc)
*DR*20	20 37 00.960	41 34 55.74	80.861	0.383	–4.44	3.98(1)	1.24	8.4	1.7(±2.1)	1.0(±2.1)
*W*75	20 38 36.428	42 37 34.82	81.871	0.781	6.76	9.8(2)	152.28			
*DR*21*B*_1	20 39 01.989	42 24 59.30	81.752	0.591	–9.07	–2.5(2)	4.00	8.6	3.0(±1.5)	
*DR*21*B*_2	20 39 01.057	42 22 49.18	81.722	0.571	–3.03	–2.5(2)	2.65	8.6	3.0(±1.5)	
*DR*21*B*_3	20 39 00.374	42 24 37.13	81.744	0.591	3.56	–2.5(2)	3.16	8.6	3.0(±1.5)	

References for the velocities: 1 – Schneider et al. (2006); 2 – Plume et al. (1992).

19120+0917. This sources exhibits multiple features that coincide in velocity with the 12.2-GHz features (Blaszkiewicz & Kus 2004).

19186+1440. This source displays multiple features at 6.7-GHz in the range from –16 to –9 km s^{-1}. Szymczak et al. (2000) also reported 6.7-GHz emission in the velocity range from −31 to −25 km s^{-1}, which was not detected in our observations.

19303+1651 and **20290+4052**. The spectra of these sources are both dominated by a single feature. Each velocity component has its 12.2-GHz counterpart (Blaszkiewicz & Kus 2004).

ON1. This source consists of two separate masing sites with a separation of around 1″. The peak velocities for these two sites are 15.7 and −0.1 km s^{-1}.

21381+5000. There is only one feature detected in the MERLIN observations, while Szymczak et al. (2000) detected multiple features.

4. Methanol masers and spiral arms

Since 6.7-GHz methanol masers appear to be exclusively associated with massive star-forming regions, they are reliable tracers of the spiral arms of the Galaxy. This is especially so since the lifetime of methanol masers is understood to be about 10^4 yr (van der Walt 2005). To investigate whether any information about the spiral structure of the Galaxy can be inferred from the data of methanol masers detected to date, we compiled a table of all known 6.7-GHz methanol masers (Table 5). The LSR velocities in Table 5 originate in molecular lines such as CS, CO, and NH_3, where such data are available. For other sources, the velocity of the maser peak was used. The kinematical distances were calculated using the Galactic rotation model of Wouterloot & Brand (1989), assuming R_0 = 8.5 kpc and Θ_0 = 220 km s^{-1}. We made no attempt to calculate the distances for those sources, which are located in the two Galactic longitude ranges 0° ± 10° and 180° ± 10°, where the uncertainty in the kinematic method is large.

A significant fraction of the sources in the first and the fourth Galactic quadrants are affected by an ambiguity between two

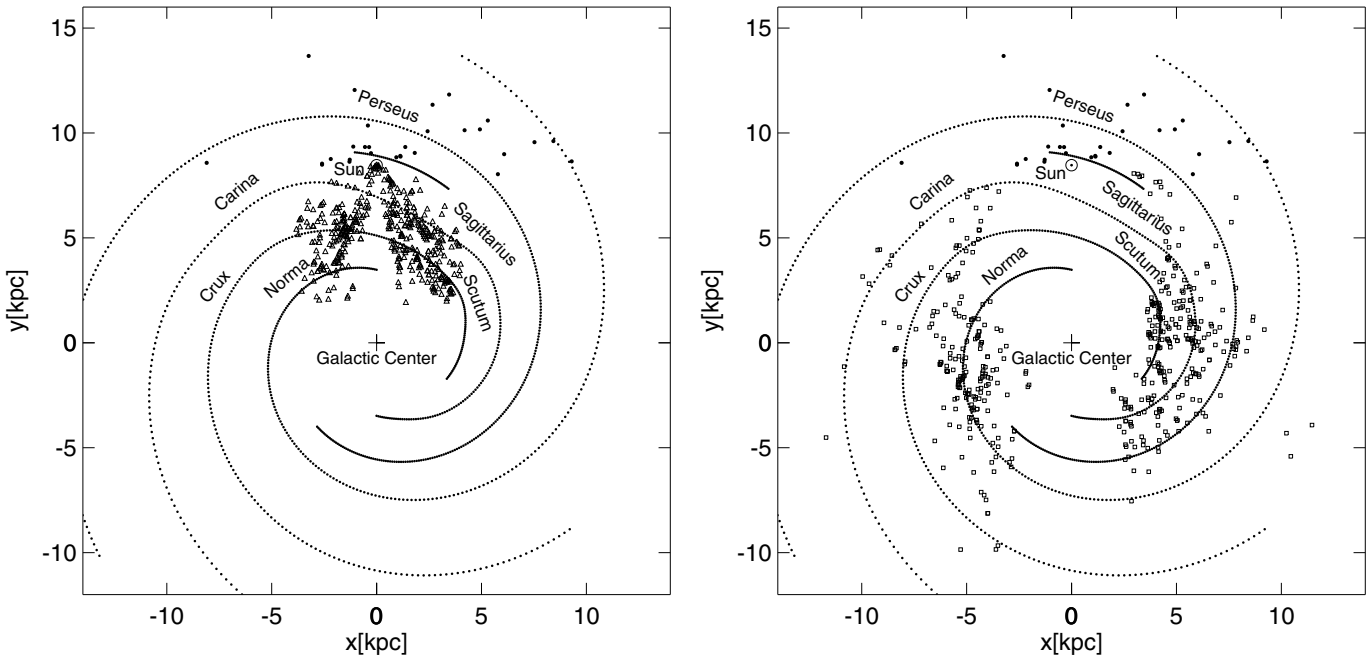

Fig. 1. Positions of 495 6.7-GHz masers at the near (open triangles), far (open squares) kinematic distances, and of the outer Galaxy (filled circles) in the Galactic plane. The distances calculated using the Galactic rotation model of Wouterloot & Brand (1989), assuming R_0 = 8.5 kpc and Θ_0 = 220 km s^{-1}. There is a poor correspondence between the spiral arm models and massive star-forming regions for both the near and far distances and also in the outer Galaxy. The positions of the spiral arms are taken from Cordes & Lazio (2002). We do not show error bars for clarity.

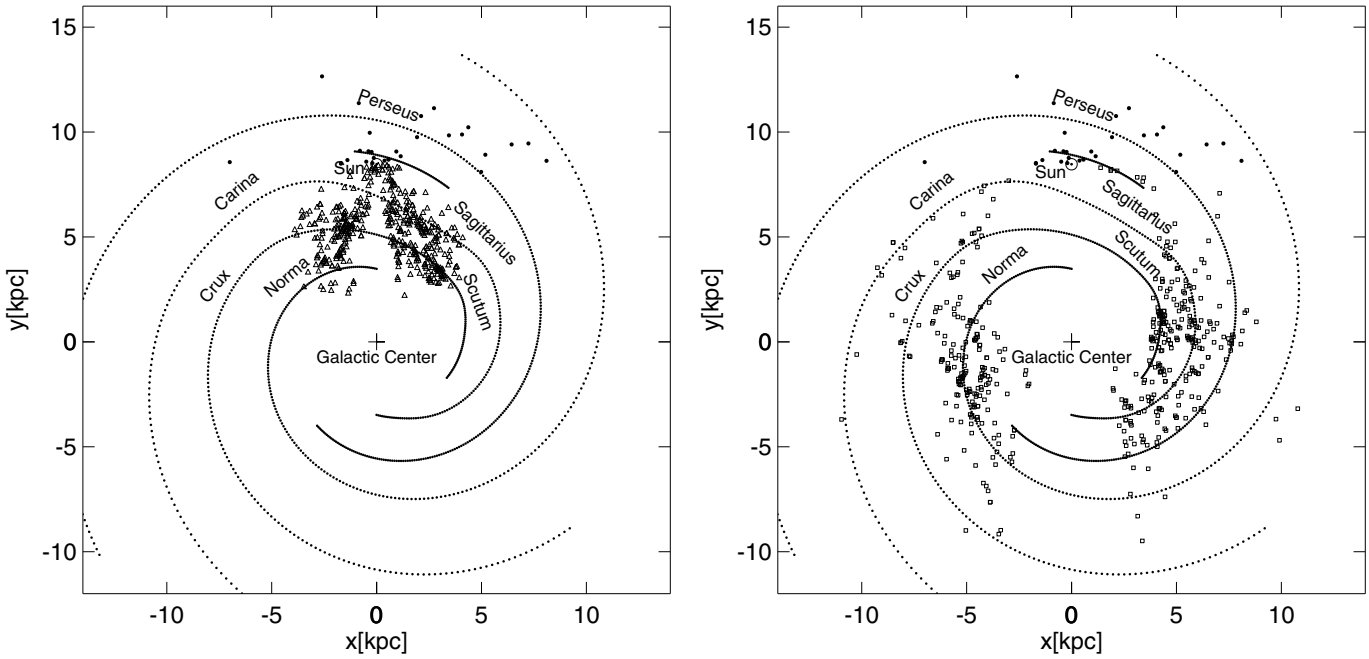

Fig. 2. Same as in Fig. 1, but the revised distances from Reid et al. (2009) have been used. There is little difference between Figs. 1 and 2 in the inner Galaxy, but there is a far closer agreement between the model and the data in the Perseus arm region of the outer Galaxy.

distances, the near and the far distance. This kinematical distance ambiguity has been resolved for only a small number of methanol masers (Pandian et al. 2008). Sobolev et al. (2005) proposed that statistically, it is preferable to assume a more nearby kinematic distance than a far distance. The left panel of Fig. 1 shows a face-on diagram of the Galaxy, where the near kinematic distance is assumed for all sources affected by a distance ambiguity. Spiral arm loci from the NE2001 model of Cordes & Lazio (2002) are superimposed. It can be seen that there is little if any correlation between the location of methanol masers

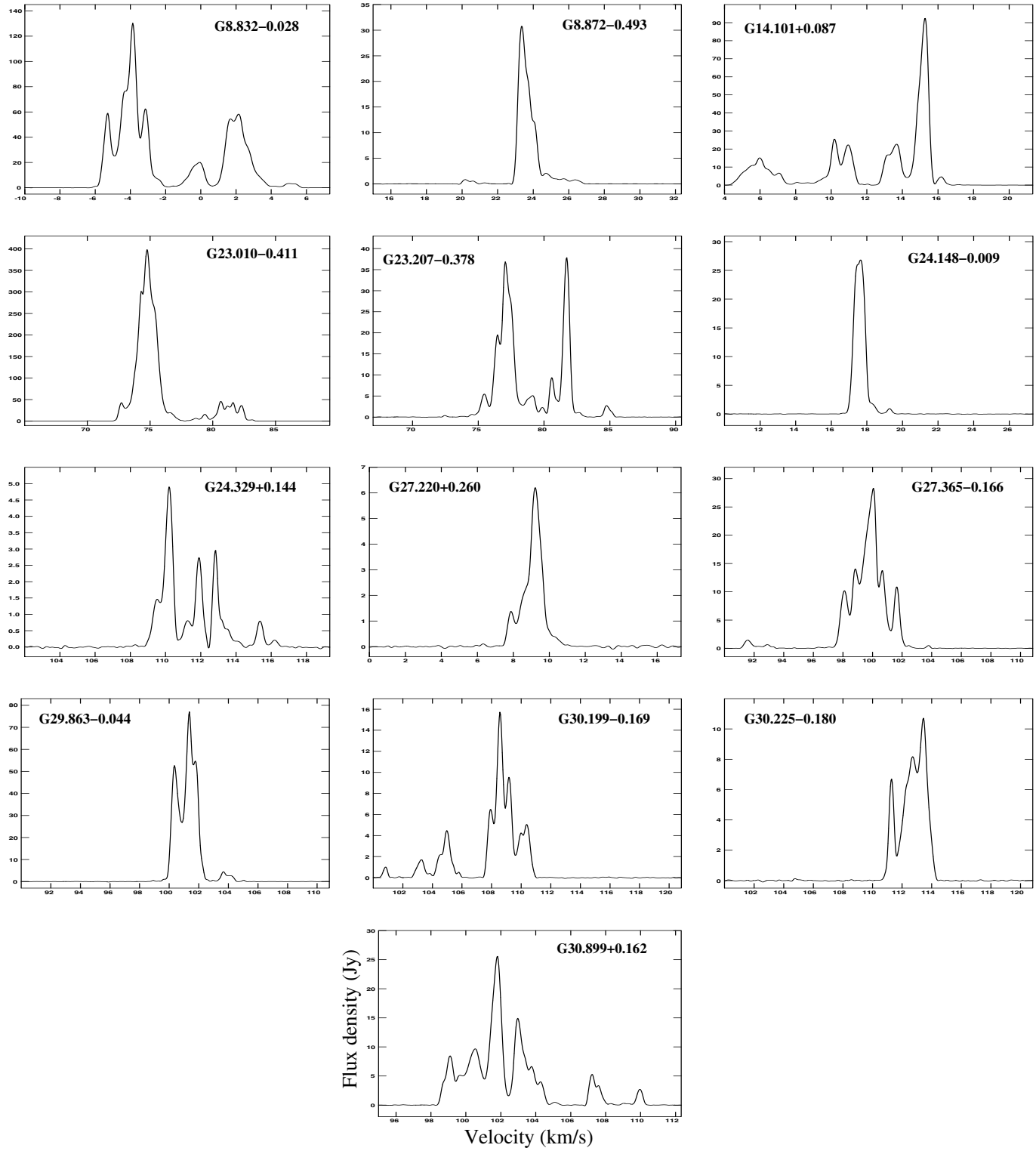

Fig. 3. Spectra of the 6.7-GHz methanol masers from the ATCA observations. The spectral resolution is approximately 0.18 km s^{-1}.

and the spiral arm model. The right panel of Fig. 1 shows the same diagram, but with the far distance being assumed for all masers affected by a distance ambiguity. Qualitatively, there appears to be a stronger correlation with the spiral arm loci in the right-hand panel than in the left-hand one. Keeping in mind that in reality there are only a fraction of sources located at the near distance, and that the kinematic distances have relatively large uncertainties, it seems possible to reconcile the spiral arm model with the distribution of methanol masers in the Galaxy. However, this exercise does suggest that the assumption of the majority of sources being at the near kinematic distance may be flawed. This suggestion can be corroborated by a general observation that the

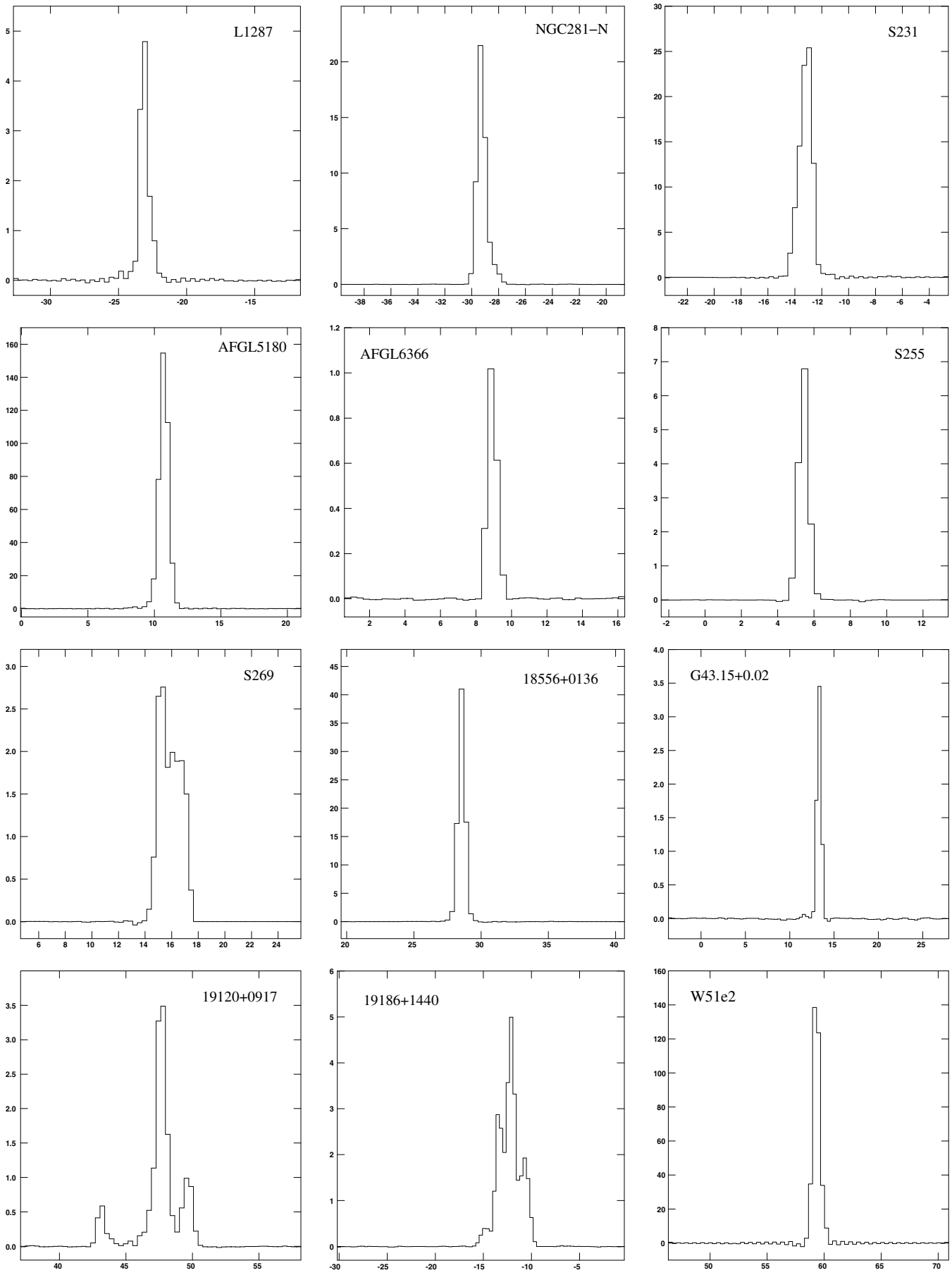

Fig. 4. Same as Fig. 3, but for the spectra obtained with the MERLIN. The spectral resolution is approximately 0.7 km s^{-1}.

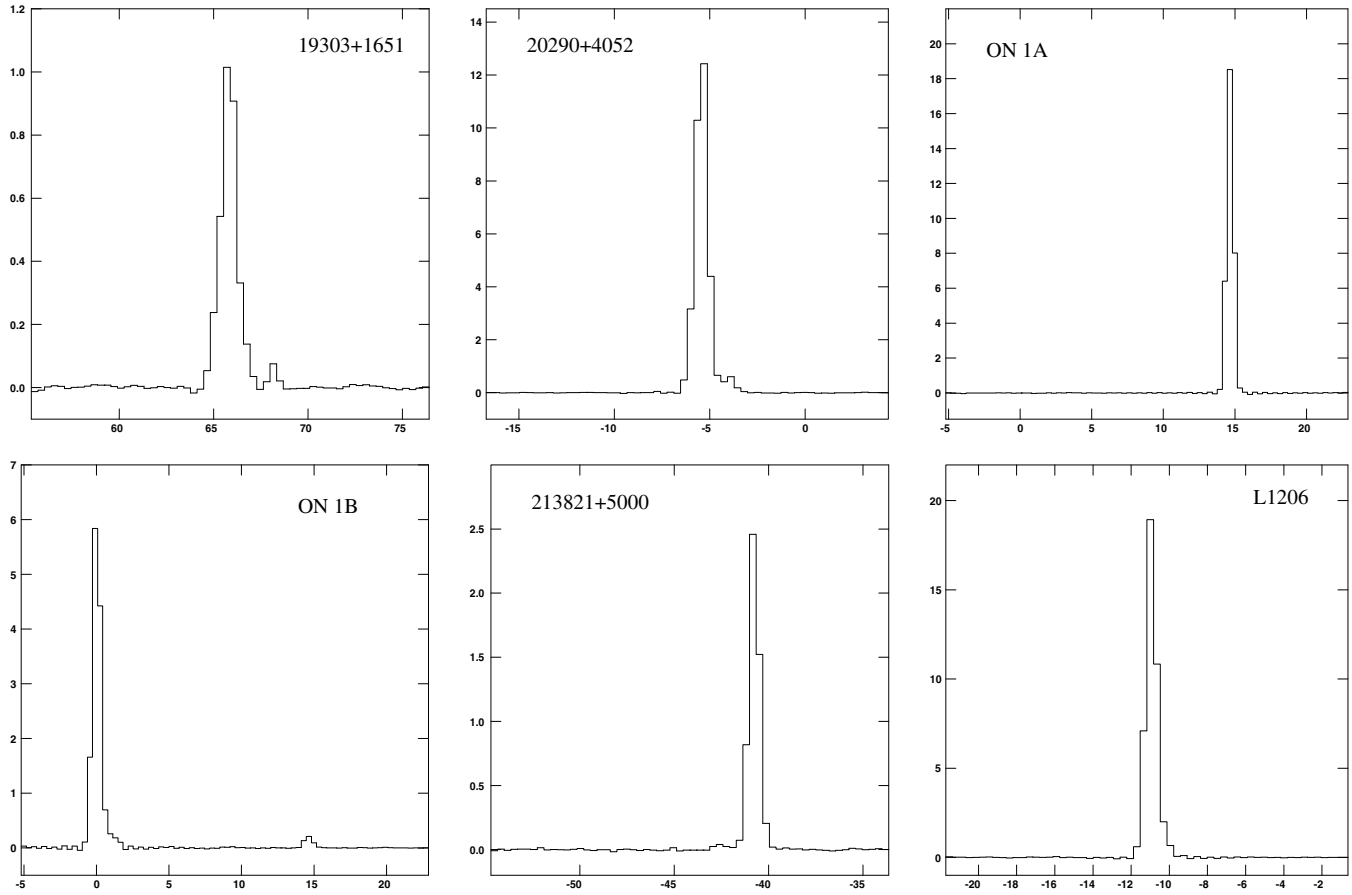

Fig. 4. continued.

majority of young massive star-forming regions associated with HII regions appear to be at the far distance in the studies able to resolve the ambiguity (e.g., Kolpak et al. 2003).

Figure 1 also shows that there is a poor correspondence between the spiral arm model and the massive star-forming regions in the outer Galaxy where there is no distance ambiguity. This is mostly caused by a significant deviation from the circular rotation in the Perseus arm region (Xu et al. 2006a). Based on the VLBI parallax measurements for a number of massive star forming-regions, Reid et al. (2009) found that these regions orbit the Galactic center ∼15 km s^{-1} slower than the Galaxy itself, if one assumes circular rotation. In addition, the motion of the Sun towards the local standard of rest (LSR) was found to be consistent with that derived by Dehnen & Binney (1998) from Hipparcos data. We hence recalculated kinematic distances using the methodology explained in Sect. 4 of Pandian et al. (2008) – the radial velocities were recalculated to the new frame of solar motion, and kinematic distances were calculated using the Galactic rotation curve of Wouterloot & Brand (1989) with R_0 = 8.4 kpc and Θ_0 = 254 km s^{-1} (Reid et al. 2009), assuming that the massive star forming-regions were rotating 15 km s^{-1} slower than predicted by the rotation curve. The left-hand and the right-hand panels of Fig. 2 show the equivalent of Fig. 1 for the new kinematic distances. It can be seen that there is little difference between Figs. 1 and 2 for the inner Galaxy, but there is now much closer agreement between the model and the data in the Perseus arm region of the outer Galaxy.

5. Association with star formation tracers

It is well established that the 6.7-GHz methanol masers are associated with high-mass stars (e.g., W3(OH); see Menten et al. 1992), which are able to pump the masers by heating a sufficient amount of surrounding dust to temperatures higher than 100 K, or producing hypercompact HII regions with extremely high emission measures (Sobolev et al. 2007). No 6.7-GHz methanol masers have been found to be associated with low-mass young stellar objects (Minier et al. 2003; Bourke et al. 2005).

Maser surveys suggest that the 6.7-GHz methanol masers are associated with different phases of development in the HII regions (Ellingsen 2007). Almost all 6.7-GHz masers are found to be associated with 1.2 mm emission (Hill et al. 2005), while many have no associated 8.6-GHz continuum emission (Walsh et al. 1998). Relevant cases can be found even within one star-forming region, e.g., NGC6334 I, which possesses a maser cluster associated with a prominent ultracompact HII region and another one associated with the sub-mm core and a candidate hypercompact HII region with very weak radio continuum emission (Hunter et al. 2006).

Maser positions measured to subarcsecond accuracy allow us to study the connection between the methanol masers and the other signposts of massive star formation. However, there are no published high resolution continuum surveys in radio or submillimeter wavelengths that cover all or a significant fraction of the sources in our sample. Hence, we focus on infrared counterparts from all sky or Galactic plane surveys.

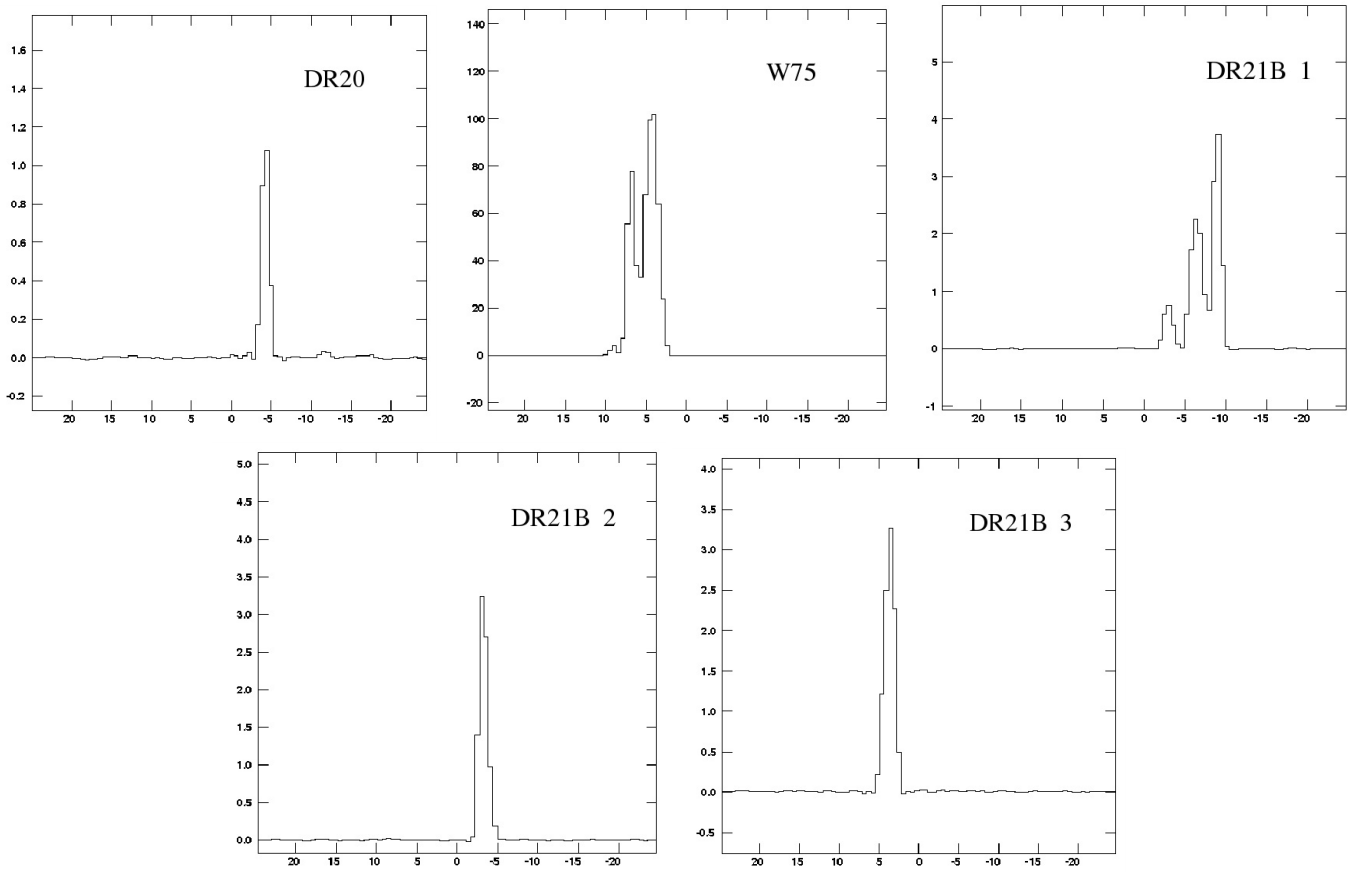

Fig. 5. Same as Fig. 3, but for the VLA spectra. The spectral resolution is approximately 0.55 km s^{-1}.

Table 4 presents the association with infrared sources. Among the 35 sources in our sample, 25 are in the inner Galaxy, while 10 are located in the outer Galaxy. In the inner Galaxy, 19 of 25 sources are covered by the GLIMPSE survey, which is limited to Galactic longitudes, $|l| \leq 65°$. Seventeen sources have a GLIMPSE point source within 5 arcsec, dropping to 11 within 2 arcsec. Most sources with no nearby point source in the GLIMPSE catalog or archive data are associated with extended emission, and one source (G23.2068-0.3777) is associated with an infrared dark cloud. Only four sources have flux measurements in all four bands (often due to extended emission in the other bands), and hence we do not attempt to compare the properties of the sources with those published previously (e.g., Ellingsen 2006).

Twenty-one masers have a 2MASS point-source counterpart within 5 arcsec, dropping to 9 within 2 arcsec. Most of the sources show an infrared excess based on their *JHK* colors, which is indicative of an association with protostars. Four sources show no infrared excess, suggesting that they are either foreground stars or more evolved objects. By Cross-correlating with the GLIMPSE catalog, only five GLIMPSE sources are found to have 2MASS counterparts. This strongly suggests that most of the 6.7-GHz methanol masers do not have 2MASS counterparts, and that most of the nearby 2MASS sources are more evolved young stellar objects in the star-forming region. This supports the results of Ellingsen (2005, 2006).

Since the black-body emission of the warm dust, hypothesized to be the pump source for the masers, peaks at around 25 μm (Ostrovskii & Sobolev 2002), one expects all methanol masers to have mid/far infrared counterparts. Two surveys with data at this wavelength range are the all sky survey of *IRAS*, and the MIPSGAL survey using the Spitzer space telescope. Keeping in mind that the *IRAS* point source catalog is limited by both source confusion and poor resolution, 20 methanol masers have an *IRAS* point source within 30 arcsec. We note that 9 of 10 sources located in the outer Galaxy, where source confusion is not as severe as in the inner Galaxy, have an *IRAS* point source with an infrared luminosity greater than 10^3 $L_\odot$. However, due to the poor resolution of the *IRAS* satellite, it is possible that a single point source in the *IRAS* catalog may correspond to multiple star-forming sites in the molecular cloud. Hence, higher spatial resolution data is required to infer properties such as the luminosity and mass of the source associated with the maser.

MIPSGAL is a Galactic plane survey at 24 and 70 μm using the MIPS camera of the Spitzer Space Telescope (Rieke et al. 2004; Carey et al. 2005). The survey is limited to Galactic longitudes between 5 and 63 degrees in the first Galactic quadrant and 298 and 355 degrees in the fourth quadrant for Galactic latitudes $|b| \leq 1°$. Eighteen sources in our sample are covered by the survey, and all sources are associated with 24 μm emission, as shown in Fig. 6. An association with point sources (which are occasionally saturated) is evident for 16 sources, while for 2 sources (G43.15+0.02 and *W*51*e*2) the images are completely saturated. It is thus reasonable to expect that all the 6.7-GHz methanol masers have MIPSGAL counterparts. However, image artifacts such as saturation make it difficult to determine 24 μm fluxes. Further observations will be required before we will be able to determine their spectral energy distributions and dust properties. Fifteen sources in our sample have an MSX point source within 5″. When restricted to sources that are covered

Table 4. Association of the 6.7-GHz methanol masers with the GLIMPSE, 2MASS, MSX, and *IRAS* point sources.

Source name	2MASS		GLIMPSE		MSX		*IRAS*	
	name	separation (arcsec)	name	separation (arcsec)	name	separation (arcsec)	name	separation (arcsec)
G8.832−0.028			GLMC G008.8315−00.0278	0.5			18024−2119	15.9
G8.872−0.493	18071532−2130540	0.4	GLMA G008.8721−00.4926	0.3	G008.8725−00.4929	2.4	18042−2131	6.9
G14.101+0.087			GLMC G014.1017+00.0872	1.7			18128−1640	11.8
G23.010−0.411			GLMC G023.0097−00.4105	0.3				
G23.207−0.378			GLMC G023.2075−00.3772	3.1				
G24.148−0.009			GLMC G024.1479−00.0091	0.3			18326−0751	11.3
G24.329+0.144			GLMC G024.3285+00.1440	0.4			18324−0737	5.2
G27.220+0.260			GLMC G027.2197+00.2607	0.9				
G27.365−0.166			GLMA G027.3650−00.1656	0.8			18391−0504	2.3
G29.863−0.044	18455955−0245061	1.8	GLMA G029.8623−00.0442	2.1	G029.8620−00.0444	3.5		
G30.199−0.169	18470306−0230361	2.6	GLMA G030.1981−00.1691	2.5	G030.1981−00.1691	2.4		
G30.225−0.180	18470824−0229302	3.3	extended emission					
G30.899+0.162			GLMC G030.8988+00.1615	1.1				
L1287	00364719+6329058	3.8					00338+6312	1.0
NGC281-N	00522425+5633471	4.0					00494+5617	4.3
S231	05391330+3545538	3.8			G173.4815+02.4459	1.4		
AFGL5180	06085340+2138281	1.3					06058+2138	12.0
AFGL6366	06084091+2131056	3.6					06056+2131	7.6
S255	06125385+1759242	2.5			G192.6005−00.0479	0.8	06099+1800	10.0
S269	06143706+1349364	0.4			G196.4542−01.6777	1.8	06117+1350	7.1
18556+0136			GLMA G035.1973−00.7430	1.1	G035.1979−00.7427	3.7	18556+0136	1.6
G43.15+0.02	19101091+0905176	3.5	GLMC G043.1480+00.0131	3.5	G043.1492+00.0130	1.1		
19120+0917	19142616+0922346	3.8	extended emission		G043.8896−00.7835	3.9	19120+0917	3.8
19186+1440			GLMC G049.4152+00.3253	2.1				
W51e2			GLMC G049.4892−00.3879	2.3				
19303+1651	19323607+1657384	0.1	GLMC G052.6625−01.0919	0.4			19303+1651	12.1
ON1A	20100886+3131392	4.8			G069.5395−00.9754	1.2	20081+3122	1.4
ON1B	20100886+3131392	4.2			G069.5395−00.9754	2.0	20081+3122	1.8
20290+4052	20305058+4102298	2.5			G079.7358+00.9905	0.9	20290+4052	2.9
21381+5000	21395825+5014209	0.1			G094.6028−01.7966	2.7	21381+5000	7.0
L1206							22272+6358A	5.8
DR20	20370116+4134545	2.6			G080.8624+00.3827	4.6	20352+4124	2.2
W75								
DR21B_1	20390200+4225008	1.6			G081.7522+00.5906	0.7		
DR21B_2	20390101+4222502	1.2			G081.7220+00.5699	4.1		
DR21B_3	20390047+4224369	1.2						

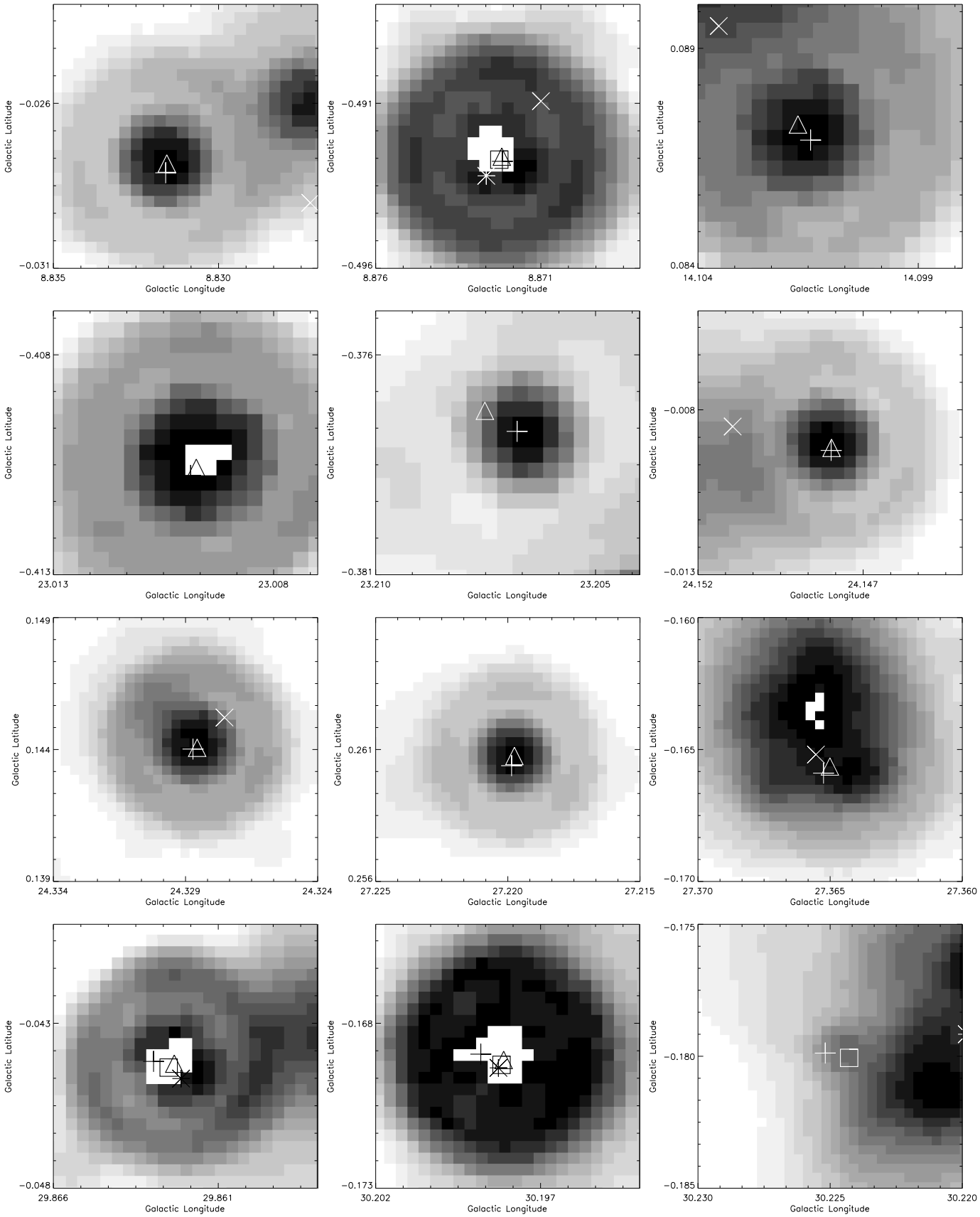

Fig. 6. Gray scale is the MIPSGAL 24 μm emission, the pluses are the positions of 6.7-GHz methanol masers, the triangles are the positions of GLIMPSE point sources, the squares are the positions of 2MASS point sources, the stars are the positions of MSX point sources, and the crosses are the positions of *IRAS* point sources. Moving *from the top left to the bottom right*, the sources are G8.8316-0.0281, G8.8722-0.4928, G14.1014+0.0869, G23.0099-0.4107, G23.2068-0.3777, G24.1480-0.0092, G24.3287+0.1440, G27.2198+0.2604, G27.3652-0.1659, G29.8630-0.0442, G30.1987-0.1687, G30.2251-0.1796, G30.8987+0.1616, 18556+0136, G43.15+0.02, 19120+0917, 19186+1440, and W51e2.

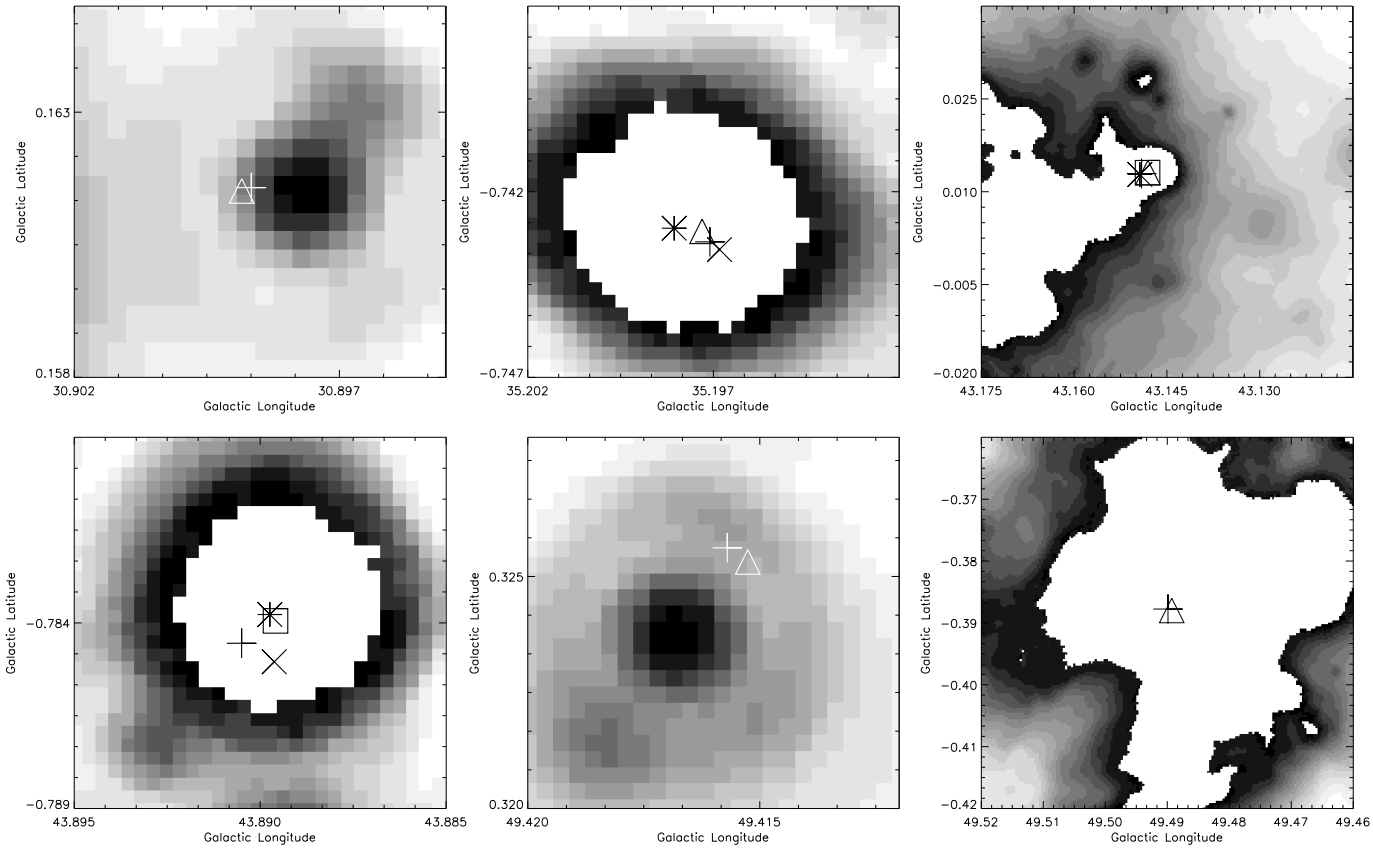

Fig. 6. continued.

by the MIPSGAL survey, only six sources have a nearby MSX source. The far poorer statistics of the associations with MSX sources is probably caused by the coarser spatial resolution of the MSX satellite and its poorer sensitivity.

6. Conclusions

Absolute positions with an accuracy of 1 arcsecond or higher have been determined for 35 6.7-GHz methanol masers. Our measurements are essential to a future VLBI astrometric follow-up observations. Kinematic distances to the masers imply that they do not trace the spiral arms well irrespective of whether they are at the near or far kinematic distances, although there is a small improvement if the rotation curve of Reid et al. (2009) is used. Although our sample is not statistically complete, the number of associations with infrared sources is consistent with the expectation that the 6.7 GHz masers are associated with the early phases of massive star formation.

Acknowledgements. We would like to thank the referee, Simon Ellingsen, for many useful suggestions and comments which help us to improve this paper. The Australia Telescope is funded by the Commonwealth of Australia for operation as a National Facility managed by CSIRO. We thank Drs. A. M. S. Richards and R. Beswick for help in reducing MERLIN data. This work was supported by the Chinese NSF through grants NSF 10673024, NSF 10733030, NSF 10703010 and NSF 10621303, and NBRPC (973 Program) under grant 2007CB815403. AMS was supported by RFBR grants 07-02-00628-a and 08-02-00933-a. This work used the NASA/IPAC Infrared Science Archive.

References

Anglada, G., Estalella, R., et al. 1996, ApJ, 463, 205
Beuther, H., & Sridharan, T. K. 2007, ApJ, 668, 348
Bourke, T. L., Hyland, A. R., & Robinson, G., 2005, ApJ, 625, 883
Blaszkiewicz, L., & Kus, A. J. 2004, A&A, 413, 233
Bronfman, L., Nyman, L.-A., & May, J. 1996, A&AS, 115, 81
Carey, S. J., Noriega-Crespo, A., Price, S. D., et al. 2005, BAAS, 37, 1252
Caswell, J. 1996a, MNRAS, 279, 79
Caswell, J. 1996b, MNRAS, 283, 606
Caswell, J. L. 2009, PASA, in press
Caswell, J. L., Vaile, R. A., Ellingsen, S. P., et al. 1995a, MNRAS, 272, 96
Caswell, J. L., Vaile, R. A., Ellingsen, S. P., et al. 1995b, MNRAS, 274, 1126
Caswell, J. L., Vaile, R. A., & Forster, J. R. 1995c, MNRAS, 277, 210
Churchwell, E., Walmsley, C. M., & Cesaroni, R. 1990, A&AS, 83, 119
Cordes, J. M., & Lazio, T. J. W. 2002 [arXiv:astro-ph/0207156]
Dehnen, W., & Binney, J. J. 1998, MNRAS, 298, 387
Diamond, P. J., & Kemball, A. J. 2003, ApJ, 599, 1372
Ellingsen, S., von Bibra, M., McCulloch, P., et al. 1996, MNRAS, 280, 378
Ellingsen, S. P. 2005, MNRAS, 359, 1498
Ellingsen, S. P. 2006, ApJ, 638, 241
Ellingsen, S. P. 2007, MNRAS, 377, 571
Felli, M., Palagi, F., & Tofani, G. 1992, A&A, 255, 293
Fontani, F., Caselli, P., et al. 2006, A&A, 460, 709
Garay, G., Moran, J. M., & Rodriguez, L. F. 1993, ApJ, 413, 582
Gaylard, M., & MacLeod, G. 1993, MNRAS, 262, 43
Hill, T., Burton, M. G., Minier, V., et al. 2005, MNRAS, 363, 405
Hunter, T. R., Brogan, C. L., Megeath, S. T., et al. 2006, ApJ, 649, 888
Juvela, M. 1996, A&AS, 118, 191
Kim, K. T., & Koo, B. C. 2003, ApJ, 596, 362
Kolpak, M. A., Jackson, J. M., Bania, T. M., Clemens, D. P., & Dickey, J. M. 2003, ApJ, 582, 756
Larionov, G. M., Val'tts, I. E., Winnberg, A., et al. 1999, A&AS, 139, 257
MacLeod, G., & Gaylard, M. 1992, MNRAS, 256, 519
MacLeod, G. C., Gaylard, M. J., & Kemball, A. J. 1993, MNRAS, 262, 343
MacLeod, G. C., van der Walt, D., North, A., et al. 1998, AJ, 116, 2936
Mauersberger, R., Henkel, C., Wilson, T. L., et al. 1986, A&A, 162, 199
Malyshev, A. V., & Sobolev, A. M. 2003, A&ATr 22, 1
Menten, K. 1991, ApJ, 380, 75
Menten, K. M., Reid, M. J., Pratap, P., Moran, J. M., & Wilson, T. L. 1992, ApJ, 401, 39
Minier, V., Booth, R., & Conway, J. 1998, A&A, 336, L5

Minier, V., Booth, R., & Conway, J. 2000, A&A, 362, 1093
Minier, V., Conway, J., & Booth, R. 2001, A&A, 369, 278
Minier, V., Ellingsen, S., Norris, R., et al. 2003, A&A, 403, 1095
Molinari, S., Brand, J., et al. 1996, A&A, 308, 573
Norris, R. P., Whiteoak, J. B., Caswell, J. L., Wieringa, M. H., & Gough, R. G. 1993, ApJ, 412, 222
Ostrovskii, A. B., & Sobolev, A. M. 2002, IAUS, 206, 183
Pandian, J. D., Goldsmith, P. F., & Deshpande, Avinash, A. 2007 ApJ, 656, 255
Pandian, J. D., Momjian, E., & Goldsmith, P. F. 2008, A&A, 486, 191
Pestalozzi, M., Minier, V., & Booth, R. 2005, A&A, 432, 737
Phillips, C. J., Norris, R. P., Ellingsen, S. P., et al. 1998, MNRAS, 300, 1131, 275
Pillai, T., Wyrowski, F., Carey, S. J., et al. 2006, A&A, 450, 569
Pirogov, L., Zinchenko, I., et al. 2003, A&A, 405, 639
Plume, R., Jaffe, D. T., Evans, N. J., II, et al. 1992, ApJS, 78, 505
Reid, M. J., Menten, K. M., Zheng, X. W., et al. 2009, ApJ, 700, 137
Rieke, G. H., Young, E. T., Engelbracht, C. W., et al. 2004, ApJS, 154, 25
Russeil, D. 2003, A&A, 397, 133
Schneider, N., Bontemps, S., Simon, R., et al. 2006, A&A, 458, 855
Schutte, A., van der Walt, D., Gaylard, M., et al. 1993, MNRAS, 261, 783
Slysh, V., Val'tts, I., & Kalenskii, S. 1999, A&AS, 134, 115
Sobolev, A. M., Ostrovskii, A. B., Kirsanova, M. S., et al. 2005, Massive Star Birth, ed. E. Churchwell, P. Conti, & M. Felli, A Crossroads of Astrophysics Proc. IAU Symp., 227
Sobolev, A. M., Cragg, D. M., Ellingsen, S. P., et al. 2007, IAUS, 242, 81
Solomon, P. M., Rivolo, A. R., Barrett, J., et al. 1987, ApJ, 319, 730
Szymczak, M., Hrynek, G., & Kus, A. J. 2000, A&AS, 143, 269
Szymczak, M., Kus, A., Hrynek, G., Kepa, A., & Pazdereski, E. 2002, MNRAS, 392, 277
Szymczak, M., Bartkiewicz, A., & Richards, A. M. S. 2007, A&A, 468, 617
Teyssier, D., Hennebelle, P., & Perault, M. 2002, A&A, 382, 624
van der Walt, D., 2005, MNRAS, 360, 153
van der Walt, D., Gaylard, M., & MacLeod, G. 1995, A&AS, 110, 81
van der Walt, D., Retief, S., Gaylard, M., & MacLeod, G. 1996, MNRAS, 282, 1085
van der Walt, D. J., Sobolev, A. M., & Butner, H. 2007, A&A, 464, 1015
Vilas-Boas, J. W. S., & Abraham, Z. 2000, A&A, 355, 1115
Walsh, A., Hylard, A., Robinson, G., & Burton, M. 1997, MNRAS, 291, 261
Walsh, A. J., Burton M. G., Hyland A. R., et al. 1998, MNRAS, 301, 640
Wouterloot, J. G. A., & Brand, J. 1989, A&AS, 80, 149
Wouterloot, J. G. A., Brand, J., & Fiegle, K. 1993, A&AS, 98, 589
Wu, Y., Zhang, Q., Yu, W., et al. 2006, A&A, 450, 607
Xu, Y., Zheng, X. W., & Jiang, D. R. 2003, Chinese J. Astron. Astrophys., 3, 49
Xu, Y., Reid, M. J., Zheng, X. W., et al. 2006a, Science, 311, 54
Xu, Y., Reid, M. J., Menten, K. M., et al. 2006b, ApJS, 166, 526
Xu, Y., Li, J. J., Hachisuka, K., et al. 2008, A&A, 485, 729
Zhang, Q., Hunter, T. R., Brand, J., et al. 2005, ApJ, 625, 864
Zinchenko, I., Mattila, K., & Toriseva, M. 1995, A&AS, 111, 95Z

Table 5. Parameters of 592 6.7-GHz methanol masers.

Source name	RA(2000) (^{h} ^{m} ^{s})	Dec(2000) ($^\circ$ $'$ $''$)	V_{LSR} (km s^{-1})	Θ_0 = 220 km s^{-1}			Θ_0 = 254 km s^{-1}			Ref.
				R (kpc)	d_{far} (kpc)	d_{near} (kpc)	R (kpc)	d_{far} (kpc)	d_{near} (kpc)	
0.21−0.00	17 46 07.66	−28 45 20.0	37.5[19]	0.2	8.7	8.3	0.2	8.6	8.2	6,43,44
0.31−0.20	17 47 09.12	−28 46 16.0	18.7[3]	0.5	9.0	8.0	0.5	8.9	7.9	6,43,44
0.37+0.04	17 46 21.42	−28 35 39.5	84.4[3]	0.1	8.6	8.4	0.1	8.5	8.3	4,6,43
0.39−0.03	17 46 41.12	−28 37 05.5	28.7[27]	0.4	8.9	8.1	0.4	8.8	8.0	6
0.49+0.18	17 46 04.00	−28 24 51.5	−3.8[3]	25.0	33.5		25.0	33.4		6,43,44
0.53+0.18	17 46 09.8	−28 23 29	−3.8[3]	25.0	33.5		25.0	33.4		32,43,33
0.54−0.85	17 50 14.53	−28 54 31.0	16.6[30]	0.9	9.4	7.6	0.9	9.3	7.5	20,4,43,44
0.64−0.04	17 47 18.65	−28 24 25.0	60.5[30]	0.3	8.8	8.2	0.3	8.7	8.1	20,4,6,43,44 33
0.66−0.02	17 47 18.61	−28 22 56.0	60.2[30]	0.3	8.8	8.2	0.3	8.7	8.1	20,4,6,33
0.67−0.02	17 47 19.23	−28 22 14.5	66.1[30]	0.3	8.8	8.2	0.3	8.7	8.1	20,4,6,33
0.69−0.03	17 47 24.81	−28 21 43.5	66.1[30]	0.3	8.8	8.2	0.3	8.7	8.1	20,4,6,43,33
0.83+0.18	17 46 52.82	−28 07 35.0	5.4[3]	3.1	11.5	5.4	3.2	11.6	5.2	6
1.14−0.12	17 48 48.47	−28 01 12.0	−15.6[3]	25.0	33.5		25.0	33.4		43,44
2.14+0.01	17 50 35.5	−27 05 55	63.0[27]	0.9	9.3	7.6	1.0	9.3	7.5	20,4
2.53+0.19	17 50 46.48	−26 39 45.0	4.5[27]	5.7	14.2	2.8	5.8	14.2	2.6	32,43,44
3.91+0.00	17 54 39.0	−25 34 48	17.0[27]	3.9	12.3	4.7	4.0	12.3	4.4	20,4
5.90−0.42	18 00 40.87	−24 04 20.5	10.5[30]	5.7	14.1	2.8	5.8	14.1	2.7	4,43,44
6.60−0.08	18 00 54.05	−23 17 02.0	1.0[27]	8.2	16.5	0.3	8.0	16.3	0.4	32,43,44
6.78−0.27	18 01 57.2	−23 12 37	21.1[3]	4.6	12.9	4.0	4.7	12.9	3.8	39,33
8.13+0.22	18 03 01.0	−21 48 47	18.6[30]	5.2	13.5	3.3	5.3	13.5	3.2	32,43
8.68−0.36	18 06 23.5	−21 37 23	33.7[41]	4.1	12.3	4.5	4.2	12.3	4.3	20,4,43
8.83−0.03	18 05 25.66	−21 19 25.5	0.5[49]	8.4	16.7	0.1	8.2	16.4	0.2	52
8.87−0.49	18 07 15.32	−21 30 54.4	23.4[52]	4.9	13.2	3.6	5.0	13.1	3.5	52
9.62+0.19	18 06 14.659	−20 31 31.57	4.3[30]	7.6	15.8	0.9	7.5	15.6	1.0	20, 4, 43, 23
9.98−0.02	18 07 50.11	−20 18 57.0	48.9[41]	3.6	11.7	5.1	3.7	11.7	4.9	32, 43, 44
10.09+0.71	18 05 18.18	−19 51 14.5	2.0[27]	8.1	16.3	0.4	7.9	16.0	0.5	43
10.32−0.26	18 09 24.2	−20 08 07	31.3[3]	4.6	12.7	4.0	4.7	12.7	3.8	33
10.32−0.15	18 09 01.46	−20 05 08.0	14.7[41]	6.1	14.3	2.4	6.1	14.2	2.3	32, 43, 44
10.44−0.01	18 08 44.9	−19 54 38	71.4[12]	2.9	10.9	5.9	3.0	10.9	5.6	20, 4, 43, 44
10.47+0.02	18 08 38.21	−19 51 49.5	67.1[30]	3.1	11.0	5.7	3.2	11.0	5.5	20, 4, 43, 44
10.62−0.29	18 10 09.9	−19 53 22	−8.0[27]	10.7	18.9		10.2	18.3		20, 4, 43
10.62−0.38	18 10 29.24	−19 55 41.5	−3.4[41]	9.3	17.5		9.0	17.1		4, 43, 44
10.89+0.14	18 09 03.3	−19 26 26	21.7[47]	5.5	13.6	3.1	5.5	13.5	3.0	35
10.95+0.02	18 09 39.3	−19 26 28	20.6[3]	5.6	13.7	3.0	5.6	13.7	2.8	32,43,44
11.03+0.06	18 09 39.7	−19 21 36	15.9[41]	6.1	14.2	2.5	6.1	14.1	2.4	4,43
11.15−0.14	18 10 28.1	−19 22 40	29.2[3]	4.9	13.0	3.7	5.0	13.0	3.5	9
11.49−1.48	18 16 22.13	−19 41 27.5	10.6[41]	6.8	14.9	1.8	6.7	14.8	1.7	32, 43, 44
11.90−0.14	18 12 11.44	−18 41 29.0	37.8[41]	4.5	12.5	4.1	4.6	12.5	3.9	20, 4, 43, 44
11.93−0.61	18 14 00.89	−18 53 26.5	38.4[3]	4.5	12.5	4.2	4.6	12.5	4.0	20, 4, 43, 44
11.99−0.27	18 12 51.20	−18 40 39.5	59.5[41]	3.6	11.4	5.2	3.7	11.5	5.0	43, 44
12.02−0.03	18 12 01.851	−18 31 55.50	109.8[3]	2.4	9.9	6.7	2.5	10.0	6.4	20, 4, 43, 44
12.20−0.10	18 12 39.92	−18 24 17.5	24.2[41]	5.5	13.5	3.1	5.5	13.4	3.0	20, 4, 43, 44
12.25−0.04	18 12 31.9	−18 20 11	48.7[27]	4.1	11.9	4.7	4.1	11.9	4.5	35
12.62+0.00	18 13 07.4	−17 59 09	21.1[3]	5.8	13.8	2.8	5.8	13.7	2.7	33
12.68−0.18	18 13 54.2	−18 01 44	55.4[30]	3.8	11.7	4.9	3.9	11.7	4.7	20,4
12.71−0.11	18 13 43.4	−17 58 06	57.7[27]	3.8	11.6	5.0	3.9	11.6	4.8	35
12.79−0.19	18 14 11.1	−17 55 57	35.7[16]	4.8	12.7	3.9	4.9	12.7	3.7	20
12.89+0.49	18 11 51.4	−17 31 30	33.7[30]	4.9	12.8	3.7	5.0	12.8	3.6	20, 4, 43, 44
12.90−0.26	18 14 39.52	−17 52 00.0	37.6[30]	4.7	12.6	4.0	4.8	12.6	3.8	20, 4, 43, 44
12.93−0.07	18 14 01.1	−17 45 05	58.7[27]	3.8	11.5	5.0	3.9	11.6	4.8	35
13.18+0.06	18 14 00.8	−17 28 05	50.8[1]	4.1	11.9	4.6	4.2	11.9	4.4	35
13.66−0.60	18 17 24.4	−17 22 13	49.9[30]	4.2	12.0	4.5	4.3	12.0	4.3	35, 51
13.70−0.05	18 15 30.2	−17 03 58	51.9[27]	4.2	11.9	4.6	4.2	11.9	4.4	35
14.09+0.10	18 15 45.80	−16 39 09.7	9.3[41]	7.2	15.1	1.3	7.1	15.0	1.3	33, 52
14.33−0.63	18 18 53.37	−16 47 39.5	22.2[30]	6.0	13.8	2.7	6.0	13.7	2.6	43
14.45−0.05	18 16 59.4	−16 24 52	27.0[27]	5.6	13.4	3.0	5.6	13.4	2.9	35
14.60+0.01	18 17 01.14	−16 14 39.0	24.4[3]	5.8	13.6	2.8	5.8	13.6	2.7	43, 44
15.03−0.67	18 20 24.79	−16 11 35.5	19.8[41]	6.2	14.0	2.4	6.2	13.9	2.3	20,4,43,44
15.08−0.09	18 18 22.7	−15 52 46	45.8[27]	4.6	12.3	4.2	4.7	12.3	4.0	35
15.67−0.48	18 20 58.3	−15 32 34	−3.4[27]	9.0	16.9		8.7	16.5		35
16.36−0.19	18 21 15.6	−14 47 33	45.0[31]	4.8	12.3	4.0	4.9	12.3	3.8	35
16.58−0.05	18 21 09.13	−14 31 48.5	59.3[41]	4.3	11.7	4.6	4.3	11.7	4.4	20, 4, 43, 44

Table 5. continued.

Source name	RA(2000) (h m s)	Dec(2000) (° ′ ″)	V_{LSR} (km s^{-1})	Θ_0 = 220 km s^{-1} R (kpc)	d_{far} (kpc)	d_{near} (kpc)	Θ_0 = 254 km s^{-1} R (kpc)	d_{far} (kpc)	d_{near} (kpc)	Ref.
16.86−2.15	18 29 24.41	−15 16 04.0	17.5[41]	6.6	14.3	2.0	6.6	14.1	2.0	4, 43, 44
17.01−2.39	18 30 33.9	−15 14 53	19.8[41]	6.4	14.1	2.2	6.4	13.9	2.1	35
17.02−0.08	18 22 08.6	−14 09 29	90.8[27]	3.4	10.5	5.8	3.5	10.5	5.5	35
17.65+0.16	18 22 25.7	−13 29 28	22.5[41]	6.3	13.8	2.4	6.3	13.7	2.3	17,4
18.06+0.08	18 23 31.3	−13 09 23	55.2[27]	4.6	11.8	4.3	4.7	11.9	4.1	35
18.15+0.10	18 23 37.2	−13 04 23	57.9[27]	4.5	11.7	4.4	4.6	11.7	4.2	35
18.26−0.27	18 25 13.3	−13 09 16	75.2[27]	4.0	11.0	5.1	4.0	11.0	4.9	35
18.34+1.78	18 17 54.1	−12 06 48	32.9[25]	5.7	13.1	3.1	5.7	13.0	2.9	39,33
18.46−0.00	18 24 36.35	−12 51 08.0	52.2[3]	4.8	12.0	4.1	4.8	12.0	3.9	20, 4, 43, 44
18.65+0.04	18 24 48.7	−12 39 17	80.2[27]	3.9	10.8	5.3	3.9	10.9	5.1	35
18.84−0.30	18 26 24.7	−12 39 10	42.5[41]	5.2	12.5	3.6	5.3	12.5	3.4	33
18.89+0.05	18 25 12.4	−12 26 16	38.2[27]	5.4	12.7	3.3	5.5	12.7	3.2	35
18.99−0.04	18 25 44.1	−12 24 15	55.4[9]	4.7	11.8	4.3	4.8	11.8	4.1	9
19.36−0.03	18 26 25.79	−12 03 53.0	26.2[25]	6.2	13.5	2.5	6.2	13.4	2.4	43,44,35
19.48+0.15	18 26 00.39	−11 52 22.5	24.4[41]	6.3	13.7	2.4	6.3	13.5	2.3	20,4,43,44,35
19.61−0.13	18 27 16.52	−11 53 38.5	57.6[41]	4.7	11.7	4.3	4.7	11.7	4.1	4,43
19.61−0.23	18 27 37.2	−11 56 27	42.7[30]	5.3	12.5	3.5	5.3	12.4	3.4	4,43,44,35
19.70−0.26	18 27 55.52	−11 52 39.0	43.6[27]	5.3	12.4	3.6	5.3	12.4	3.4	35,44
19.88−0.52	18 29 11.7	−11 49 58	43.6[3]	5.3	12.4	3.6	5.3	12.4	3.4	35
20.08−0.13	18 28 10.32	−11 28 47.0	41.9[30]	5.4	12.5	3.5	5.4	12.5	3.3	20,4,43,44,36
20.24+0.08	18 27 41.0	−11 14 05	71.0[41]	4.3	11.1	4.9	4.4	11.1	4.6	20,4,35,36
21.41−0.25	18 31 06.3	−10 21 37	90.7[37]	3.9	10.2	5.6	4.0	10.3	5.3	35,36
21.57−0.03	18 30 36.5	−10 06 44	97.7[25]	3.7	10.0	5.9	3.8	10.1	5.6	35,36
21.87+0.01	18 31 01.75	−09 49 01.0	22.4[3]	6.6	13.7	2.1	6.6	13.6	2.0	20,4,43,44,35
22.05+0.22	18 30 35.7	−09 34 26	50.0[34]	5.2	12.0	3.8	5.2	12.0	3.6	35,36
22.34−0.16	18 32 32.1	−09 29 10	30.9[37]	6.1	13.1	2.6	6.1	13.0	2.6	36
22.36+0.06	18 31 44.13	−09 22 12.5	84.6[41]	4.1	10.4	5.3	4.2	10.5	5.0	32,43,44,35,36
22.43−0.16	18 32 41.2	−09 24 34	28.7[41]	6.3	13.2	2.5	6.2	13.1	2.4	20,4,35,36
22.45−0.17	18 32 45.8	−09 24 06	29.5[27]	6.2	13.2	2.5	6.2	13.1	2.5	36
23.01−0.41	18 34 40.29	−09 00 38.1	74.8[16]	4.4	10.8	4.9	4.5	10.8	4.6	20,4,52
23.04−0.32	18 34 26.2	−08 56 35	76.0[31]	4.4	10.7	4.9	4.5	10.8	4.7	35,36
23.18−0.45	18 35 08.1	−08 52 32	75.2[27]	4.4	10.7	4.9	4.5	10.8	4.7	35
23.19−0.38	18 34 55.20	−08 49 14.2	81.8[27]	4.3	10.5	5.2	4.3	10.5	4.9	35,36,52
23.24−0.24	18 34 31.26	−08 42 47.0	63.2[41]	4.8	11.3	4.3	4.9	11.3	4.1	32,43,44,33,35,36
23.32−0.29	18 34 49.9	−08 40 34	63.8[27]	4.8	11.2	4.4	4.9	11.3	4.2	35
23.39+0.19	18 33 13.1	−08 23 56	74.1[27]	4.5	10.8	4.8	4.6	10.8	4.6	35,36
23.43−0.18	18 34 39.27	−08 31 39.0	104.2[3]	3.8	9.5	6.1	3.9	9.6	5.8	20,4,43,44,35,36
23.48+0.08	18 33 44.05	−08 21 20.5	84.4[3]	4.2	10.3	5.3	4.3	10.4	5.0	32,43,44,33,35
23.66−0.13	18 34 51.7	−08 18 16	82.3[27]	4.3	10.4	5.2	4.4	10.5	4.9	36
23.70−0.19	18 35 12.37	−08 17 39.5	68.9[37]	4.7	11.0	4.6	4.7	11.0	4.4	32,43,44,33,35
23.80+0.40	18 33 13.0	−07 55 41	76.4[27]	4.5	10.6	4.9	4.5	10.7	4.7	35
23.91+0.07	18 34 38.2	−07 59 35	35.7[48]	6.0	12.7	2.9	6.0	12.6	2.8	48
23.98−0.08	18 35 22.9	−08 01 11	72.7[37]	4.6	10.8	4.8	4.6	10.8	4.5	35,36
24.14+0.00	18 35 20.94	−07 48 55.6	23.1[37]	6.7	13.5	2.0	6.6	13.3	2.0	35,36,52
24.33+0.14	18 35 08.14	−07 35 04.0	112.0[16]	3.7	8.9	6.6	3.8	9.2	6.1	20,4,35,36,52
24.50−0.03	18 36 08.7	−07 30 55	109.8[30]	3.7	9.0	6.5	3.8	9.2	6.0	39,33,35,36
24.54+0.32	18 34 53.0	−07 19 11	107.8[37]	3.8	9.1	6.4	3.9	9.3	6.0	35,36
24.64−0.33	18 37 25.2	−07 31 53	42.7[37]	5.7	12.2	3.2	5.7	12.2	3.1	36
24.67−0.14	18 36 48.4	−07 24 25	113.0[3]	3.7	8.8	6.7	3.8	9.1	6.2	33,35
24.78+0.08	18 36 12.57	−07 12 11.5	110.7[41]	3.8	8.9	6.5	3.8	9.2	6.1	20,4,43,44,35
24.92+0.10	18 36 24.0	−07 04 27	109.3[27]	3.8	8.9	6.5	3.9	9.2	6.0	35
24.93+0.08	18 36 29.2	−07 05 05	53.4[27]	5.3	11.6	3.8	5.3	11.6	3.6	36
25.38+0.00	18 37 35.52	−06 42 34.5	95.7[27]	4.1	9.6	5.8	4.2	9.7	5.4	8
25.38−0.18	18 38 14.3	−06 47 47	68.2[7]	4.8	10.9	4.5	4.9	10.9	4.3	48
25.41+0.10	18 37 16.92	−06 38 28.0	96.0[37]	4.1	9.6	5.8	4.2	9.7	5.5	39,8,35,36
25.53+0.38	18 36 32.6	−06 24 26	92.0[27]	4.2	9.7	5.6	4.3	9.9	5.3	8
25.65+1.04	18 34 20.91	−05 59 40.5	42.2[25]	5.8	12.2	3.2	5.8	12.1	3.0	39,44,33,35
25.70+0.04	18 38 03.15	−06 24 15.0	101.3[15]	4.0	9.2	6.1	4.1	9.4	5.7	8,43,44,35,36
25.82−0.17	18 39 03.63	−06 24 09.5	91.2[27]	4.2	9.7	5.6	4.3	9.9	5.3	32,8,43,44,35,36
26.52−0.26	18 40 40.23	−05 49 07.5	104.2[31]	4.0	8.9	6.3	4.1	9.2	5.9	8
26.59−0.00	18 39 52.8	−05 38 48	23.3[37]	6.8	13.3	1.9	6.7	13.1	1.9	35,36
26.60−0.22	18 40 38.55	−05 43 56.0	107.8[41]	3.9	8.6	6.6	4.0	9.0	6.1	39,33,8,35,36

Table 5. continued.

Source name	RA(2000) (^{h} ^{m} ^{s})	Dec(2000) ($^\circ$ $'$ $''$)	V_{LSR} (km s^{-1})	Θ_0 = 220 km s^{-1} R (kpc)	d_{far} (kpc)	d_{near} (kpc)	Θ_0 = 254 km s^{-1} R (kpc)	d_{far} (kpc)	d_{near} (kpc)	Ref.
26.65+0.02	18 39 51.8	−05 34 52	111.5[3]	3.9	8.3	6.9	4.0	8.7	6.3	35,36
27.21+0.26	18 40 03.72	−04 57 45.6	9.1[27]	7.8	14.3	0.8	7.6	14.0	0.9	36,52
27.22+0.13	18 40 30.43	−05 00 59.0	112.6[37]	3.9	7.9	7.3	4.0	8.5	6.4	8,36
27.28+0.15	18 40 34.48	−04 57 13.5	31.8[41]	6.4	12.6	2.5	6.4	12.5	2.4	8,33,35,36
27.36−0.16	18 41 50.98	−05 01 28.0	92.2[41]	4.3	9.4	5.7	4.4	9.6	5.3	20,4,8,35,36,52
27.78+0.05	18 41 47.5	−04 33 11	111.8[27]	4.0	7.8	7.3	4.0	8.4	6.4	35
27.78−0.25	18 42 57.2	−04 41 59	45.7[3]	5.8	11.8	3.3	5.8	11.7	3.2	35,36
27.86−0.24	18 43 01.1	−04 36 41	20.1[7]	7.1	13.4	1.7	7.0	13.2	1.7	48
28.02−0.44	18 44 02.1	−04 34 14	16.0[27]	7.3	13.6	1.4	7.2	13.4	1.4	36
28.14+0.00	18 42 42.59	−04 15 32.0	100.9[27]	4.2	8.7	6.2	4.3	9.0	5.8	4,44,8,36
28.20−0.05	18 42 58.20	−04 13 59.5	96.8[16]	4.3	9.0	6.0	4.4	9.2	5.6	20,4,43,35,36
28.30−0.38	18 44 21.99	−04 17 38.5	48.1[3]	5.7	11.6	3.4	5.7	11.5	3.3	32,8,43,44,33,36
28.39+0.08	18 42 54.5	−04 00 04	79.2[28]	4.7	9.9	5.0	4.8	10.0	4.7	35,36
28.53+0.12	18 42 57.7	−03 51 59	27.1[27]	6.7	12.8	2.1	6.6	12.7	2.1	36
28.69+0.41	18 42 13.6	−03 35 07	94.2[27]	4.4	9.1	5.8	4.5	9.3	5.5	36
28.81+0.36	18 42 37.49	−03 30 12.5	87.0[37]	4.6	9.5	5.4	4.6	9.6	5.1	8,36
28.82+0.48	18 42 12.43	−03 25 39.5	83.3[27]	4.7	9.7	5.2	4.7	9.8	4.9	8
28.83−0.25	18 44 51.09	−03 45 48.0	86.5[30]	4.6	9.5	5.4	4.6	9.6	5.1	20,4,8,44,35,36
28.84−0.23	18 44 47.1	−03 44 39	86.5[30]	4.6	9.5	5.4	4.6	9.6	5.1	36
28.85+0.50	18 42 12.8	−03 24 26	83.5[27]	4.7	9.6	5.2	4.7	9.8	4.9	35,36
28.86+0.07	18 43 45.1	−03 35 29	103.8[30]	4.2	8.3	6.6	4.3	8.7	6.0	4,43
29.31−0.16	18 45 24.97	−03 17 44.5	45.5[27]	5.9	11.6	3.2	5.9	11.5	3.1	8,36
29.86−0.04	18 45 59.57	−02 45 04.4	100.4[41]	4.3	8.3	6.5	4.4	8.7	5.9	4,8,36,52
29.91−0.05	18 46 05.9	−02 42 27	104.3[48]	4.2	7.7	7.1	4.3	8.4	6.2	8
29.91−0.03	18 46 03.69	−02 41 52.5	97.4[3]	4.4	8.5	6.2	4.5	8.8	5.7	48
29.92+0.05	18 45 44.18	−02 39 03.5	99.0[27]	4.4	8.4	6.3	4.4	8.7	5.8	8
29.95−0.02	18 46 03.741	−02 39 21.43	97.3[41]	4.4	8.5	6.2	4.5	8.8	5.7	20,4,8,43,44,36,23
29.98−0.04	18 46 11.6	−02 38 42	97.3[41]	4.4	8.5	6.2	4.5	8.8	5.7	4,36
30.00−0.01	18 46 09.85	−02 36 30.5	97.7[15]	4.4	8.5	6.2	4.5	8.8	5.8	8
30.20−0.17	18 47 03.07	−02 30 33.6	103.3[41]	4.3	7.7	7.0	4.4	8.3	6.2	4,36,52
30.22−0.18	18 47 08.30	−02 29 27.1	104.5[41]	4.3	7.7	7.0	4.3	8.2	6.3	4,36,52
30.30+0.06	18 46 23.7	−02 17 56	45.3[37]	6.0	11.5	3.2	5.9	11.4	3.1	35,36
30.30−0.18	18 47 18.6	−02 25 40	102.6[3]	4.3	7.8	6.9	4.4	8.4	6.1	35
30.40−0.29	18 47 51.2	−02 23 15	102.4[37]	4.3	7.7	6.9	4.4	8.4	6.1	36
30.53+0.01	18 47 00.1	−02 07 26	48.0[41]	5.9	11.3	3.3	5.9	11.3	3.2	43
30.59−0.13	18 47 37.5	−02 08 46	115.5[27]							36
30.59−0.04	18 47 18.89	−02 06 07.0	42.3[41]	6.1	11.6	3.0	6.1	11.5	2.9	20,4,35,44,36
30.70−0.07	18 47 36.9	−02 01 05	88.8[16]	4.6	9.0	5.7	4.7	9.2	5.3	20,4,35,36
30.76−0.05	18 47 39.73	−01 57 22.0	90.5[30]	4.6	8.8	5.8	4.7	9.0	5.4	20,4,43,44,35,36
30.78+0.23	18 46 41.52	−01 48 32.0	41.6[41]	6.1	11.6	3.0	6.1	11.6	2.9	20,35
30.78+0.00	18 47 29.9	−01 54 39	95.1[3]	4.5	8.5	6.1	4.6	8.8	5.7	4,44,35,36
30.79+0.20	18 46 48.09	−01 48 46.0	86.0[27]	4.7	9.1	5.5	4.8	9.3	5.1	4,44,36
30.82+0.27	18 46 37.4	−01 45 14	97.6[16]	4.5	8.2	6.4	4.5	8.6	5.8	20,4,35,36
30.82−0.05	18 47 46.2	−01 54 14	98.7[30]	4.4	8.1	6.5	4.5	8.5	5.9	20,4,43,35,36
30.86+0.16	18 47 09.13	−01 44 10.5	102.0[27]	4.4	7.7	6.9	4.4	8.2	6.2	43,44,52
30.91+0.14	18 47 15.0	−01 44 07	104.0[27]	4.4	7.7	6.9	4.4	8.0	6.4	32
30.94+0.11	18 47 23.8	−01 42 39	101.5[27]	4.4	7.4	7.1	4.4	8.3	6.2	35
30.96−0.14	18 48 19.7	−01 48 59	74.8[27]	5.0	9.8	4.8	5.1	9.8	4.6	36
30.98−0.05	18 48 05.8	−01 45 36	74.7[27]	5.0	9.8	4.8	5.1	9.8	4.6	35
31.04+0.36	18 46 41.5	−01 30 42	77.6[37]	4.9	9.6	5.0	5.0	9.7	4.7	35,36
31.06+0.09	18 47 41.34	−01 37 21.5	38.4[3]	6.3	11.8	2.8	6.2	11.7	2.7	32,43,44,35,36
31.16+0.06	18 47 59.6	−01 32 37	38.9[37]	6.3	11.7	2.8	6.2	11.7	2.7	35
31.28+0.06	18 48 12.39	−01 26 22.6	109.9[3]				4.4	7.5	6.8	20,4,43,44,35,36,23
31.41+0.31	18 47 34.31	−01 12 47.0	97.0[30]	4.5	8.0	6.5	4.6	8.5	5.9	32,4,43,44,35,36
31.58+0.08	18 48 44.3	−01 11 18	96.0[37]	4.5	8.1	6.4	4.6	8.5	5.8	35,36
32.03+0.06	18 49 37.3	−00 45 47	96.0[30]	4.6	7.9	6.5	4.6	8.3	5.9	39,35,36
32.11+0.09	18 49 36.7	−00 41 05	96.5[3]	4.6	7.8	6.6	4.6	8.3	5.9	33
32.74−0.08	18 51 22.8	−00 12 15	36.9[30]	6.4	11.6	2.7	6.4	11.5	2.6	20,4,35,36
32.80+0.19	18 50 31.1	−00 01 54	15.0[3]	7.5	13.1	1.2	7.4	12.9	1.3	48
32.97+0.04	18 51 23.0	+00 03 46	83.4[37]	4.9	8.8	5.5	5.0	9.0	5.1	39,33,35,36
33.09−0.07	18 51 58.9	+00 07 27	78.1[16]	5.1	9.1	5.1	5.1	9.3	4.8	4,35,36
33.13−0.09	18 52 07.1	+00 07 56	78.1[16]	5.1	9.1	5.1	5.1	9.3	4.8	20,4,35,36

Table 5. continued.

Source name	RA(2000) (^{h} ^{m} ^{s})	Dec(2000) ($^\circ$ $'$ $''$)	V_{LSR} (km s^{-1})	Θ_0 = 220 km s^{-1} R (kpc)	d_{far} (kpc)	d_{near} (kpc)	Θ_0 = 254 km s^{-1} R (kpc)	d_{far} (kpc)	d_{near} (kpc)	Ref.
33.40+0.01	18 52 10.6	+00 25 09	74.6[16]	5.2	9.3	4.9	5.2	9.4	4.6	33,35,36
33.64−0.21	18 53 28.7	+00 31 58	61.5[37]	5.6	10.0	4.1	5.6	10.1	3.9	36
33.68−0.26	18 53 45.2	+00 32 47	62.6[27]	5.5	10.0	4.2	5.5	10.0	4.0	35
33.74−0.15	18 53 26.9	+00 39 01	53.6[27]	5.8	10.5	3.7	5.8	10.5	3.5	36
33.86+0.01	18 53 05.2	+00 49 36	64.0[27]	5.5	9.8	4.3	5.5	9.9	4.1	36
33.97−0.00	18 53 24.1	+00 55 13	61.1[37]	5.6	10.0	4.1	5.6	10.0	3.9	35,36
34.10+0.01	18 53 31.9	+01 02 26	55.9[27]	5.8	10.3	3.8	5.8	10.3	3.6	36
34.24+0.13	18 53 21.5	+01 13 43	58.9[30]	5.7	10.1	4.0	5.7	10.1	3.8	20,4,35,36
34.39+0.24	18 53 21.5	+01 24 09	57.2[25]	5.7	10.2	3.9	5.7	10.2	3.7	32,35,36
34.74−0.09	18 55 03.4	+01 34 17	51.1[37]	6.0	10.5	3.5	5.9	10.4	3.4	36
34.78−1.38	18 59 44.7	+01 01 12	45.8[3]	6.2	10.8	3.2	6.1	10.7	3.1	39,33,35
34.82+0.35	18 53 37.4	+01 50 32	56.9[11]	5.8	10.1	3.9	5.8	10.1	3.7	26
35.02+0.35	18 54 00.6	+02 00 50	52.5[16]	5.9	10.3	3.6	5.9	10.3	3.5	20,4,35,36
35.18−0.74	18 58 09.8	+01 39 36	35.0[10]	6.6	11.4	2.5	6.5	11.3	2.5	9
35.20−0.74	18 58 13.053	+01 40 35.68	35.0[30]	6.6	11.4	2.5	6.5	11.3	2.5	20,4 35,22,52
35.20−1.74	19 01 45.6	+01 13 28	43.6[3]	6.3	10.8	3.1	6.2	10.8	3.0	20,4
35.25−0.24	18 56 30.9	+01 57 11	72.4[26]	5.3	9.0	4.9	5.3	9.1	4.6	26
35.39+0.02	18 55 51.2	+02 11 37	96.9[26]				4.9	7.3	6.4	26
35.40+0.03	18 55 51.1	+02 12 25	89.1[26]	4.9	7.1	6.7	5.0	7.8	5.9	26
35.59+0.06	18 56 04.3	+02 23 28	49.6[3]	6.1	10.4	3.4	6.0	10.4	3.3	26
35.79−0.17	18 57 16.1	+02 27 44	61.9[37]	5.7	9.6	4.2	5.7	9.6	4.0	36
36.02−0.20	18 57 45.8	+02 39 15	93.0[26]				4.9	6.8	6.7	26
36.10+0.56	18 55 15.6	+03 04 42	76.0[37]	5.3	8.5	5.2	5.3	8.7	4.9	35,36
36.64−0.21	18 58 55.9	+03 12 05	77.3[26]	5.3	8.2	5.4	5.3	8.4	5.1	26
36.70+0.09	18 58 00.9	+03 23 30	59.8[37]	5.8	9.5	4.1	5.8	9.6	3.9	36
36.84−0.02	18 58 39.3	+03 27 55	61.7[26]	5.7	9.3	4.2	5.7	9.4	4.0	26
36.90−0.41	19 00 08.6	+03 20 35	84.7[26]	5.1	7.0	6.6	5.1	7.6	5.8	26
36.92+0.48	18 57 00.7	+03 46 01	−35.9[26]	11.8	17.4		11.0	16.5		26
37.02−0.03	18 58 59.9	+03 37 40	80.1[37]	5.2	7.7	5.8	5.2	8.1	5.4	36
37.38−0.09	18 59 52.3	+03 55 12	70.6[26]	5.5	8.6	4.9	5.5	8.7	4.6	26
37.40+1.52	18 54 10.5	+04 40 49	43.7[25]	6.3	10.4	3.1	6.3	10.4	3.0	32,35
37.47−0.11	19 00 06.7	+03 59 27	59.1[37]	5.8	9.4	4.1	5.8	9.4	3.9	36
37.52−0.10	19 00 14.4	+04 02 35	52.9[3]	6.0	9.8	3.7	6.0	9.8	3.5	35,36
37.54+0.21	18 59 11.6	+04 12 08	85.1[25]	5.2	7.2	6.3	5.1	7.1	6.2	33,35,36
37.60+0.42	18 58 28.5	+04 20 34	90.0[37]				5.1	7.1	6.2	36
37.74−0.12	19 00 38.0	+04 13 18	50.3[26]	6.1	9.9	3.5	6.1	9.9	3.4	26
37.76−0.19	19 00 56.5	+04 12 08	55.1[26]	6.0	9.6	3.8	5.9	9.6	3.7	26
37.77−0.22	19 01 03.0	+04 12 13	61.5[3]	5.8	9.2	4.3	5.8	9.2	4.1	26
38.03−0.30	19 01 50.0	+04 23 54	55.7[27]	5.9	9.5	3.9	5.9	9.5	3.7	36
38.08−0.27	19 01 48.4	+04 27 25	67.5[26]	5.6	8.6	4.7	5.6	8.7	4.5	26
38.10−0.21	19 01 47.6	+04 30 32	83.5[3]	5.3	7.2	6.2	5.2	7.0	6.2	35,36
38.20−0.08	19 01 22.8	+04 39 10	79.8[27]	5.3	7.0	6.4	5.3	7.6	5.6	36
38.26−0.08	19 01 28.7	+04 42 02	15.4[27]	7.6	12.2	1.2	7.4	11.9	1.3	36
38.26−0.20	19 01 54.0	+04 38 38	70.2[26]	5.5	8.3	5.0	5.5	8.5	4.7	26
38.56+0.15	19 01 10.3	+05 04 26	31.5[26]	6.9	11.0	2.3	6.8	10.9	2.3	26
38.60−0.21	19 02 34.0	+04 56 40	62.6[26]	5.8	8.9	4.4	5.8	8.9	4.2	26
38.66+0.08	19 01 36.7	+05 07 42	−31.5[26]	11.1	16.4		10.5	15.6		26
38.92−0.36	19 03 39.7	+05 09 36	40.2[25]	6.5	10.4	2.9	6.5	10.3	2.8	35,26
39.10+0.48	19 00 59.5	+05 42 28	23.1[37]	7.2	11.5	1.7	7.1	11.3	1.8	36
39.54−0.38	19 04 53.5	+05 41 59	47.8[26]	6.3	9.7	3.4	6.2	9.7	3.3	26
39.39−0.14	19 03 45.3	+05 40 39	65.8[3]	5.7	8.4	4.7	5.7	8.5	4.5	26
40.28−0.22	19 05 42.1	+06 26 08	74.0[27]	5.5	6.8	6.2	5.5	7.4	5.4	27,35,26
40.41+0.70	19 02 37.9	+06 58 25	12.0[3]	7.8	12.0	0.9	7.6	11.7	1.0	32,35
40.62−0.14	19 06 01.7	+06 46 25	32.9[16]	6.9	10.5	2.4	6.8	10.4	2.4	20,4,35
40.94−0.04	19 06 16.1	+07 06 00	36.6[26]	6.7	10.2	2.7	6.6	10.1	2.6	26
41.08−0.13	19 06 49.3	+07 11 01	57.5[26]	6.0	8.6	4.2	6.0	8.7	4.0	26
41.12−0.22	19 07 15.4	+07 10 54	63.4[27]	5.8	8.1	4.7	5.8	8.2	4.5	35,26
41.12−0.11	19 06 50.7	+07 13 57	36.6[26]	6.7	10.1	2.7	6.7	10.0	2.6	26
41.16−0.20	19 07 15.1	+07 13 20	63.6[26]	5.8	8.0	4.8	5.8	8.1	4.5	26
41.23−0.20	19 07 21.9	+07 17 06	57.1[27]	6.0	8.6	4.2	6.0	8.6	4.0	35,26
41.27+0.37	19 05 24.6	+07 35 02	20.3[26]	7.4	11.2	1.5	7.3	11.0	1.6	26
41.34−0.14	19 07 21.870	+07 25 17.34	14.0[27]	7.7	11.7	1.1	7.6	11.4	1.2	27

Table 5. continued.

Source name	RA(2000) (h m s)	Dec(2000) (° ′ ″)	V_{LSR} (km s^{-1})	Θ_0 = 220 km s^{-1} R (kpc)	d_{far} (kpc)	d_{near} (kpc)	Θ_0 = 254 km s^{-1} R (kpc)	d_{far} (kpc)	d_{near} (kpc)	Ref.
41.58+0.04	19 07 09.4	+07 42 19	11.9[26]	7.8	11.8	0.9	7.6	11.5	1.0	26
41.87−0.10	19 08 10.8	+07 54 04	15.8[26]	7.6	11.5	1.2	7.5	11.2	1.3	26
42.07+0.24	19 07 20.8	+08 14 12	12.5[27]	7.8	11.7	1.0	7.6	11.4	1.1	27
42.30−0.30	19 09 44.2	+08 11 33	28.1[26]	7.1	10.5	2.1	7.0	10.3	2.1	26
42.43−0.26	19 09 50.2	+08 19 32	65.6[3]	5.8	7.2	5.3	5.8	7.5	4.9	26
42.70−0.15	19 09 55.8	+08 36 56	−42.9[26]	12.1	16.9		11.3	15.9		26
43.04−0.46	19 11 39.7	+08 46 32	58.0[25]	6.1	8.0	4.5	6.0	8.0	4.3	35,26,51
43.08−0.08	19 10 22.4	+08 59 01	10.2[26]	7.9	11.6	0.8	7.7	11.3	0.9	26
43.15+0.02	19 10 11.049	+09 05 20.49	2.9[3]	8.3	12.2	0.2	8.1	11.8	0.4	20,4,27,52
43.18−0.01	19 10 20.2	+09 06 06	12.1[16]	7.8	11.5	0.9	7.7	11.2	1.1	26
43.80−0.13	19 11 55.1	+09 36 00	44.3[30]	6.5	8.9	3.3	6.5	8.9	3.2	20,4,35,27
43.87−0.77	19 14 26.393	+09 22 36.53	54.2[3]	6.2	8.1	4.2	6.2	8.1	4.0	35,52
44.31+0.04	19 12 16.4	+10 07 44	55.7[26]	6.2	7.7	4.4	6.1	7.8	4.2	26
44.64−0.52	19 14 54.6	+10 10 02	49.3[26]	6.4	8.3	3.8	6.3	8.3	3.7	26
45.07+0.13	19 13 22.4	+10 50 45	58.9[30]	6.1	7.0	5.0	6.1	7.1	4.7	20,4,35,27
45.44+0.07	19 14 17.4	+11 08 45	58.0[3]	6.1	6.9	5.0	6.1	7.1	4.7	4,35
45.47+0.13	19 14 07.8	+11 12 01	61.8[16]	6.1	6.4	5.5	6.0	6.3	5.5	20,4,35,27
45.49+0.13	19 14 10.1	+11 13 05	61.8[3]	6.1	6.4	5.6	6.0	6.2	5.5	4
45.57−0.12	19 15 13.2	+11 10 25	1.6[26]	8.4	11.8	0.1	8.2	11.4	0.4	26
45.81−0.36	19 16 31.9	+11 16 22	59.9[26]	6.1	6.4	5.4	6.1	6.5	5.2	26
46.07+0.22	19 14 55.6	+11 46 12	23.3[26]	7.4	10.0	1.8	7.2	9.8	1.9	26
46.12+0.38	19 14 26.4	+11 53 24	59.0[26]	6.2	6.4	5.3	6.1	6.5	5.1	26
48.89−0.17	19 21 47.5	+14 04 58	57.3[26]				6.3	6.0	5.1	26
48.90−0.27	19 22 10.1	+14 02 38	72.0[26]							26
48.99−0.30	19 22 26.3	+14 06 37	71.6[26]							26
49.03−1.06	19 25 18.5	+13 46 59	38.7[3]	6.8	7.9	3.2	6.7	7.8	3.2	39,35
49.27+0.31	19 20 44.8	+14 38 29	−3.2[26]	8.7	11.4		8.4	10.9	0.0	26
49.35+0.41	19 20 33.2	+14 45 48	68.0[26]							26
49.41+0.33	19 20 59.212	+14 46 49.65	−12.4[27]	9.2	12.1		8.9	11.6		35,26,52
49.47−0.37	19 23 39.821	+14 31 04.47	60.9[30]							20,4,23
49.48−0.40	19 23 46.1	+14 29 38	56.3[16]				6.4	5.5	5.4	26
49.49−0.39	19 23 43.949	+14 30 34.44	56.5[30]							4,52
49.60−0.25	19 23 26.7	+14 40 19	62.8[27]							35,26
49.57−0.38	19 23 53.6	+14 34 54	59.3[27]							35
49.62−0.36	19 23 52.8	+14 38 10	49.3[26]	6.5	6.1	4.9	6.4	6.2	4.7	26
49.66−0.45	19 24 19.7	+14 38 02	68.8[3]							33
50.00+0.59	19 21 10.5	+15 25 42	−5.0[27]	8.8	11.3		8.5	10.9		35
50.29+0.69	19 21 22.2	+15 43 43	25.8[3]	7.3	8.8	2.1	7.2	8.5	2.2	35
50.78+0.15	19 24 17.2	+15 53 54	49.1[26]	6.6	5.8	4.9	6.5	5.9	4.8	26,51
52.66−1.09	19 32 36.071	+16 57 38.46	59.7[3]							40,52
52.92+0.41	19 27 35.2	+17 54 26	39.1[26]	6.9	6.4	3.9	6.8	6.2	3.9	26
53.04+0.11	19 28 55.7	+17 52 01	5.0[3]	8.3	9.8	0.4	8.0	9.4	0.7	35,26
53.14+0.07	19 29 17.5	+17 56 24	23.8[27]	7.5	8.1	2.1	7.3	7.9	2.2	35,26
53.62+0.04	19 30 22.6	+18 20 28	24.1[25]	7.4	8.0	2.1	7.3	7.7	2.2	35,26
58.75+0.65	19 38 43.9	+23 07 54	32.9[3]	7.3	4.8	4.0	7.2	4.7	4.0	35
59.78+0.06	19 43 11.2	+23 44 03	22.3[30]	7.6	6.1	2.4	7.4	5.7	2.7	20,4,35,23
59.84+0.66	19 40 59.4	+24 04 39	34.9[25]							32,33
60.56−0.17	19 45 48.8	+24 17 22	4.9[3]	8.3	7.9	0.5	8.0	7.5	0.8	35
69.52−0.97	20 10 09.047	+31 31 35.06	11.7[30]	8.0	4.0	2.0				20,52
70.12+1.72	20 00 49.6	+33 28 20	−21.4[3]	9.5	8.1		9.1	7.4		33,35
71.51−0.38	20 12 56.8	+33 30 05	16.4[47]							35
73.04+1.80	20 08 04.6	+35 58 47	0.7[25]	8.5	4.9	0.1	8.2	4.1	0.8	33,35
75.76+0.34	20 21 40.1	+37 25 37	−1.2[30]	8.5	4.4		8.3	3.5	0.6	20,35
78.10+3.64	20 14 26.044	+41 13 33.39	−3.2[16]	8.6	4.1		8.3	3.2	0.3	17,33,35,22,23
78.62+0.98	20 27 26.8	+40 07 50	−39.0[27]	10.5	8.0		9.9	7.2		27
78.89+0.71	20 29 24.9	+40 11 21	−6.2[16]	8.8	4.3		8.5	3.5		48
79.75+0.99	20 30 50.673	+41 02 27.55	−1.4[3]	8.6	3.3		8.3	1.9	1.1	40,52
80.85+0.43	20 36 47.8	+41 36 30	−3.1[3]	8.6	3.4		8.3	2.2	0.5	33
81.72+0.57	20 39 01.057	+42 22 49.18	−2.5[30]	8.6	3.0		8.3	1.4	1.0	20,52
81.76+0.59	20 39 01.989	+42 24 59.30	−3.2[30]	8.6	3.2		8.3	1.9	0.5	20,52
81.87+0.78	20 38 36.452	+42 37 36.06	9.8[30]							20,23,52

Table 5. continued.

Source name	RA(2000) (h m s)	Dec(2000) (° ′ ″)	V_{LSR} (km s^{-1})	Θ_0 = 220 km s^{-1} R (kpc)	d_{far} (kpc)	d_{near} (kpc)	Θ_0 = 254 km s^{-1} R (kpc)	d_{far} (kpc)	d_{near} (kpc)	Ref.
85.40−0.00	20 54 13.710	+44 54 07.85	−29.5[27]	9.9	5.8		9.4	5.0		27
90.90+1.50	21 09 03.7	+50 01 13	−70.5[27]	12.7	9.3		11.7	8.1		35
94.58−1.79	21 39 58.263	+50 14 20.96	−45.6[30]	10.8	6.1		10.2	5.2		33,52
97.52+3.17	21 32 13.0	+55 52 56	−71.1[3]	12.8	8.5		11.8	7.3		48
98.02+1.44	21 42 58.1	+54 55 46	−63.9[3]	12.2	7.6		11.3	6.5		35
106.80+5.31	22 19 18.3	+63 18 48	−15.5[48]	9.2	1.9		8.8	1.2		48
108.18+5.51	22 28 51.408	+64 13 41.30	−9.9[25]	8.9	1.2		8.6	0.6		33,52
108.75−0.96	22 58 40.3	+58 46 05	−50.3[3]	11.3	5.2		10.6	4.3		35
109.86+2.10	22 56 18.095	+62 01 49.45	−10.2[30]	9.0	1.2		8.6	0.6		20,35,23
109.92+1.98	22 57 11.2	+61 56 03	−8.7[46]	8.9	1.0		8.6	0.4		33
110.21+2.62	22 57 05.2	+62 37 44	−2.7[51]	8.6	0.3		8.3			51
111.24−0.76	23 16 05.4	+59 55 22	−44.7[3]	11.0	4.5		10.3	3.7		35
111.53+0.76	23 13 45.364	+61 28 10.55	−55.7[30]	11.8	5.7		11.0	4.7		20,21,23
121.28+0.65	00 36 47.358	+63 29 02.18	−17.6[30]	9.4	1.6		9.0	1.1		51,33,52
123.05−6.31	00 52 24.196	+56 33 43.17	−31.8[30]	10.4	2.9		9.8	2.3		33,52
133.94+1.04	02 27 03.849	+61 52 25.42	−47.4[30]	12.3	4.8		11.4	3.8		20,33,35
136.84+1.12	02 49 23.1	+60 46 26	−39.8[3]	11.7	3.9		10.9	3.1		33
168.06+0.82	05 17 13.3	+39 22 14	−25.4[25]	19.8	11.4		16.8	8.5		48
173.49+2.42	05 39 13.059	+35 45 51.29	−15.8[30]	24.1	15.6		19.4	11.1		20,22,52
173.69+2.87	05 41 33.8	+35 48 27	−19.2[30]	25.0	16.6		25.0	16.7		40,35
173.71+2.35	05 39 27.6	+35 30 58	−13.5[16]	20.0	11.5		16.7	8.4		20
174.19−0.09	05 30 42.0	+33 47 14	−3.5[3]	10.2	1.7		9.5	1.1		13,33,35
183.34−0.59	05 51 06.0	+25 45 45	−9.6[46]				4.9			33,35
188.79+1.02	06 09 06.5	+21 50 26	−0.7[3]	9.1	0.7		8.1			35
188.95+0.89	06 08 53.342	+21 38 29.09	3.1[3]	9.4	0.9		9.1	0.7		20,4,35,23,52
189.03+0.76	06 08 40.671	+21 31 06.89	2.5[3]	9.2	0.7		8.9	0.5		4,33,35
189.78+0.34	06 08 34.5	+20 38 50	9.4[30]	11.5	3.0		10.8	2.5		20,4,35
192.60−0.05	06 12 54.006	+17 59 23.21	8.2[30]	10.3	1.9		9.9	1.5		20,4,22,23,52
196.45−1.68	06 14 37.051	+13 49 36.16	17.9[3]	12.1	3.7		11.3	3.0		20,4,23,52
203.32+2.05	06 41 09.7	+09 29 35	7.6[16]	9.4	0.9		9.0	0.6		20
206.54−16.4	05 41 44.15	−01 54 44.9	5.0[46]	9.0	0.6		8.7	0.3		24
212.06−0.74	06 47 12.9	+00 26 07	45.0[3]	14.1	6.1		12.9	4.9		48
213.70−12.6	06 07 47.87	−06 22 57.0	10.4[30]	9.3	1.0		9.0	0.7		20,4,43,44,35,23
232.62+0.99	07 32 09.79	−16 58 12.5	16.6[3]	9.4	1.4		9.0	1.0		17,4,43,44,35
259.94−0.04	08 35 31.09	−40 38 24.0	7.7[3]	8.8	1.3		8.5	0.5		43,44
263.25+0.52	08 48 47.85	−42 54 28.0	12.0[3]	9.0	2.2		8.7	1.4		32,43,44
264.29+1.46	08 56 24.8	−43 06 05	5.5[3]	8.7	1.3		8.4	0.2		4,43
269.15−1.13	09 03 32.3	−48 28 00	10.3[3]	8.9	2.6		8.6	1.7		4,43
269.45−1.47	09 03 14.85	−48 55 11.5	59.7[45]	11.8	8.1		11.0	7.0		43,44
270.25+0.84	09 16 41.4	−47 55 46	9.3[3]	8.9	2.6		8.6	1.7		4,43
284.35−0.42	10 24 10.0	−57 52 38	5.7[50]	8.7	5.0		8.4	4.3		4
285.35−0.00	10 32 09.62	−58 02 04.5	−2.0[3]	8.4	4.2	0.3	8.2	3.1	1.3	39,43,44
287.37+0.64	10 48 04.44	−58 27 01.0	0.9[3]	8.5	5.2		8.3	4.5	0.5	4,39,43,44
290.37+1.66	11 12 16.1	−58 46 18	−18.5[3]							4,43
290.41−2.91	10 57 33.98	−62 59 03.0	−16.5[3]	8.0	3.7	2.3				43,44
291.27−0.70	11 11 53.37	−61 18 23.5	−23.4[3]							43,44
291.58−0.43	11 15 06.4	−61 09 37	13.5[50]	9.1	7.7		8.8	7.1		13,4
293.82−0.74	11 32 05.61	−62 12 25.5	32.9[3]	10.2	10.1		9.7	9.3		43,44
293.95−0.89	11 32 43.14	−62 23 02.5	32.0[31]	10.2	10.0		9.7	9.3		43
294.51−1.62	11 35 32.22	−63 14 42.5	−15.4[3]	7.9	5.0	2.1	7.7	4.1	2.9	17,4,43,44
294.98−1.71	11 39 22.85	−63 28 26.0	−8.1[29]	8.2	6.3	0.9	7.9	5.7	1.4	43,44
296.90−1.31	11 56 50.1	−63 32 11	20.0[27]	9.5	9.6		9.1	8.9		40
298.22−0.33	12 09 59.73	−62 49 19.0	35.0[50]	10.5	11.3		9.9	10.5		4
298.26+0.74	12 11 47.66	−61 46 21.0	−30.0[27]	7.5	4.4	3.7				43,44
299.01+0.12	12 17 24.6	−62 29 04	18.0[27]	9.4	9.9		9.0	9.3		13,4,43,44
300.51−0.17	12 30 03.58	−62 56 49.0	28.4[3]	10.1	11.2		9.6	10.5		13,4,43,44
300.96+1.14	12 34 53.25	−61 39 40.5	−43.0[3]							13,4,43,44
301.14−0.23	12 35 36.9	−63 02 48	−39.4[3]							4,43
302.03−0.06	12 43 31.96	−62 55 09.5	−35.4[3]	7.2	5.1	3.9	7.1	4.7	4.2	32,43,44
305.20+0.01	13 11 16.91	−62 45 55.5	−35.6[3]	7.0	6.1	3.7	6.9	5.8	3.9	4,43,44
305.21+0.21	13 11 14.4	−62 34 26	−41.0[3]	7.0	5.4	4.4	6.9	5.4	4.3	4

Table 5. continued.

Source name	RA(2000) (^{h} ^{m} ^{s})	Dec(2000) ($^\circ$ $'$ $''$)	V_{LSR} (km s^{-1})	Θ_0 = 220 km s^{-1}			Θ_0 = 254 km s^{-1}			Ref.
				R (kpc)	d_{far} (kpc)	d_{near} (kpc)	R (kpc)	d_{far} (kpc)	d_{near} (kpc)	
305.25+0.25	13 11 33.6	−62 31 52	−32.0[27]	7.2	6.7	3.1	7.0	6.4	3.3	4
305.36+0.15	13 12 35.89	−62 37 18.5	−38.5[29]	6.9	5.4	4.5	6.9	5.4	4.4	13,4,44
305.55+0.01	13 14 21.5	−62 44 24	−39.0[3]	6.9	5.4	4.5	6.9	5.7	4.1	43
305.80−0.24	13 16 43.4	−62 58 15	−33.1[3]	7.1	6.8	3.2	7.0	6.5	3.3	4,43
305.89+0.00	13 17 18.4	−62 43 14	−34.3[3]	7.1	6.6	3.3	7.0	6.4	3.5	39
306.33−0.34	13 21 27.6	−63 00 48	−20.0[31]	7.6	8.3	1.7	7.4	8.0	1.9	4,43
308.74+0.55	13 40 51.23	−61 45 28.0	−48.1[3]	6.6	5.7	4.9	6.6	5.5	5.0	39
308.92+0.12	13 43 03.14	−62 09 00.0	−50.9[14]	6.6	6.0	4.7				4
309.39−0.14	13 47 27.72	−62 18 25.0	−50.0[27]	6.6	6.0	4.8	6.5	5.9	4.7	4
309.92+0.47	13 50 41.85	−61 35 11.0	−58.7[14]							4,43,44
310.13+0.75	13 51 54.2	−61 16 18	−55.3[3]							39
310.17−0.11	13 54 00.59	−62 06 22.0	9.3[3]	9.0	11.7		8.7	11.2		43
311.62+0.29	14 04 54.11	−61 20 08.5	−56.2[3]	6.4	5.8	5.5	6.3	6.0	5.1	43
311.64−0.38	14 06 38.82	−61 58 24.0	35.1[3]	10.9	14.5		10.3	13.7		17,4,43,44
311.96+0.14	14 07 56.3	−61 23 01	−42.2[14]	6.7	7.9	3.5	6.6	7.8	3.5	4
312.10+0.26	14 08 49.3	−61 13 26	−50.0[27]	6.4	7.0	4.4	6.4	7.0	4.3	40,43,44
312.59+0.04	14 13 15.00	−61 16 54.5	−62.7[3]							17,4,43,44
313.46+0.19	14 19 41.01	−60 51 48.0	−4.7[3]	8.2	11.3	0.4	8.0	10.9	0.6	17,4,43,44
313.57+0.32	14 20 05.4	−60 42 40	−46.5[3]	6.5	8.0	3.7	6.4	7.9	3.7	39
313.76−0.86	14 25 01.62	−61 44 58.0	−51.3[3]	6.4	7.5	4.2	6.3	7.5	4.1	43,44
313.78−0.89	14 25 12.6	−61 46 14	−48.0[27]	6.5	7.9	3.9	6.4	7.8	3.8	32
314.26+0.11	14 25 59.1	−60 39 55	−51.9[3]	6.3	7.7	4.2	6.3	7.6	4.1	3243
316.35−0.36	14 43 11.21	−60 17 14.0	−1.2[3]	8.4	12.2	0.1	8.2	11.8	0.3	43,44
316.38−0.38	14 43 23.8	−60 17 43	−2.6[14]	8.4	12.1	0.2	8.1	11.7	0.4	32,4
316.41−0.31	14 43 22.9	−60 13 09	−1.2[3]	8.4	12.2	0.1	8.2	11.8	0.3	17,4
316.64−0.08	14 44 18.43	−59 55 12.0	−20.3[14]	7.5	10.8	1.5	7.3	10.6	1.6	4,43,44
316.81−0.06	14 45 26.44	−59 49 16.5	−38.1[14]	6.7	9.6	2.8	6.6	9.4	2.8	17,4,43,44
317.47−0.41	14 51 22.5	−59 51 07	−37.7[9]	6.7	9.8	2.8	6.6	9.6	2.8	9
317.70+0.10	14 51 08.1	−59 17 32	−42.6[3]	6.5	9.5	3.1	6.5	9.3	3.1	39
318.05+0.08	14 53 44.3	−59 09 14	−50.2[14]	6.3	9.0	3.7	6.2	8.9	3.6	13,4,43
318.05−1.40	14 59 10.5	−60 28 00	46.0[27]	12.5	17.5		11.6	16.4		4,43
318.77−0.15	14 59 35.32	−59 01 21.5	−36.6[3]	6.7	10.1	2.7	6.6	10.0	2.7	43
318.94−0.19	15 00 55.40	−58 58 53.5	−35.0[27]	6.8	10.3	2.5	6.7	10.1	2.6	4,43,44
319.84−0.20	15 06 57.1	−58 33 02	−9.0[27]	8.0	12.3	0.7	7.8	12.0	0.9	4,43
320.12−0.50	15 10 00.13	−58 40 16.0	−8.7[3]	8.0	12.4	0.7	7.8	12.0	0.9	43,44
320.23−0.29	15 09 51.96	−58 25 38.0	−66.2[3]	5.7	8.2	4.8	5.7	8.3	4.6	17,4,43,44
321.03−0.48	15 15 52.52	−58 11 07.5	−61.0[27]	5.8	8.9	4.3	5.8	8.9	4.1	32,43,44
321.15−0.53	15 16 49.2	−58 09 49	−66.0[27]	5.7	8.5	4.7	5.7	8.6	4.5	13,4
321.71+1.17	15 13 46.5	−56 25 18	−41.3[3]	6.5	10.4	2.9	6.4	10.3	2.9	4,43
322.16+0.64	15 18 34.3	−56 38 10	−63.0[27]	5.7	9.0	4.4	5.7	9.1	4.2	17,4
323.45−0.07	15 29 19.32	−56 31 22.5	−67.5[3]	5.5	9.0	4.6	5.5	9.1	4.4	4,43,44
323.74−0.26	15 31 45.41	−56 30 50.0	−49.5[14]	6.1	10.3	3.4	6.0	10.2	3.3	4,43,44
324.72+0.34	15 34 59.2	−55 27 21	−47.0[27]	6.1	10.6	3.3	6.1	10.5	3.2	13,4
324.92−0.56	15 39 57.62	−56 04 07.5	−73.8[3]	5.3	8.9	5.0	5.3	9.0	4.7	43,44
326.47+0.70	15 43 18.0	−54 07 57	−40.9[3]	6.3	11.3	2.9	6.2	11.2	2.8	39,8
326.64+0.61	15 44 33.24	−54 05 30.5	−38.8[3]	6.4	11.4	2.8	6.3	11.3	2.7	32
326.64−0.60	15 49 42.7	−55 02 44	−40.0[27]	6.3	11.4	2.8	6.3	11.2	2.8	8,43,44
326.66+0.52	15 45 02.9	−54 09 03	−41.0[3]	6.3	11.3	2.9	6.2	11.2	2.8	8
326.85−0.67	15 51 14.2	−54 58 04	−57.6[3]	5.7	10.4	3.9	5.7	10.3	3.7	8
327.11+0.51	15 47 32.72	−53 52 38.0	−83.6[3]	4.9	8.8	5.5	4.9	8.9	5.2	17,4,8,43,44
327.29−0.58	15 53 07.9	−54 37 15	−53.0[42]	5.8	10.7	3.6	5.8	10.6	3.5	4
327.39+0.19	15 50 18.5	−53 57 06	−84.6[27]	4.9	8.8	5.5	4.9	9.0	5.2	8
327.40+0.44	15 49 19.5	−53 45 14	−79.7[3]	5.0	9.1	5.2	5.0	9.2	4.9	4,8,43
327.59−0.09	15 52 36.8	−54 03 18	−86.3[27]	4.8	8.7	5.6	4.8	8.9	5.3	8
327.61−0.11	15 52 50.2	−54 03 00	−97.5[27]	4.6	7.6	6.8	4.6	8.1	6.1	8
327.94−0.11	15 54 33.9	−53 50 44	−51.7[27]	5.8	10.9	3.5	5.8	10.8	3.4	8
328.23−0.54	15 57 58.28	−53 59 22.5	−44.9[27]	6.1	11.3	3.2	6.0	11.2	3.1	4,8,43,44
328.80+0.63	15 55 48.37	−52 43 06.0	−42.3[3]	6.1	11.5	3.0	6.1	11.4	2.9	4,8,43,44
328.95+0.56	15 56 49.50	−52 40 26.5	−93.0[3]	4.6	8.6	6.0	4.6	8.8	5.6	43
329.02−0.20	16 00 33.3	−53 13 02	−43.4[14]	6.1	11.5	3.1	6.0	11.4	3.0	4,8

Table 5. continued.

Source name	RA(2000) (h m s)	Dec(2000) (° ′ ″)	V_{LSR} (km s^{-1})	Θ_0 = 220 km s^{-1}			Θ_0 = 254 km s^{-1}			Ref.
				R (kpc)	d_{far} (kpc)	d_{near} (kpc)	R (kpc)	d_{far} (kpc)	d_{near} (kpc)	
329.03−0.19	16 00 30.7	−53 12 35	−43.4[14]	6.1	11.5	3.1	6.0	11.4	3.0	4,8
329.06−0.30	16 01 09.9	−53 16 02	−42.6[3]	6.1	11.5	3.0	6.1	11.5	3.0	8
329.18−0.31	16 01 45.0	−53 11 40	−55.7[27]	5.6	10.8	3.8	5.6	10.8	3.6	17,4,8
329.33+0.14	16 00 33.11	−52 44 39.5	−107.1[3]	4.3	7.6	7.0	4.3	7.7	6.8	8,43,44
329.40−0.46	16 03 30.65	−53 10 00.5	−75.0[3]	5.0	9.8	4.8	5.0	9.9	4.6	17,4,8,44
329.46+0.50	15 59 40.71	−52 23 27.5	−67.6[3]	5.2	10.2	4.4	5.2	10.2	4.2	32,8,43,44
329.61+0.11	16 02 06.7	−52 36 32	−60.1[27]	5.4	10.6	4.0	5.4	10.6	3.9	39,8
330.07+1.05	16 00 18.0	−51 35 08	−50.0[3]	5.8	11.3	3.5	5.7	11.2	3.4	39
330.88−0.37	16 10 21.21	−52 06 12.0	−62.8[14]	5.3	10.7	4.2	5.3	10.7	4.0	4,43
330.95−0.18	16 09 52.36	−51 54 57.5	−92.5[14]	4.4	9.1	5.8	4.5	9.3	5.4	13,4,8,43,44
331.12−0.11	16 10 23.17	−51 45 19.2	−93.2[27]	4.4	9.1	5.8	4.5	9.3	5.5	5,8
331.13−0.24	16 10 59.77	−51 50 22.5	−87.0[3]	4.6	9.5	5.4	4.6	9.6	5.1	17,4,5,8,43,44
331.27−0.18	16 11 26.56	−51 41 56.5	−89.3[14]	4.5	9.3	5.6	4.6	9.5	5.3	4,5,8,43,44
331.33−0.29	16 12 12.15	−51 44 12.5	−67.4[27]	5.1	10.5	4.4	5.1	10.5	4.2	17,4,8,43,44
331.42+0.26	16 10 09.4	−51 16 04	−88.6[27]	4.5	9.4	5.5	4.6	9.5	5.2	8
331.44−0.18	16 12 12.56	−51 35 11.1	−88.5[27]	4.5	9.4	5.5	4.6	9.6	5.2	39,5,8
331.54−0.06	16 12 08.81	−51 25 47.0	−91.0[42]	4.4	9.3	5.6	4.5	9.4	5.3	4,5,8
331.55−0.12	16 12 27.22	−51 27 37.0	−100.7[3]	4.2	8.7	6.3	4.3	8.9	5.8	17,4,5,8,43
332.09−0.42	16 16 16.49	−51 18 25.0	−61.4[27]	5.2	10.9	4.1	5.2	10.9	3.9	8,44
332.29+2.26	16 05 44.5	−49 12 20	−24.0[27]	6.8	13.1	2.0	6.7	12.9	2.0	39
332.29−0.09	16 15 45.4	−50 55 53	−48.4[3]	5.7	11.6	3.4	5.7	11.6	3.3	8
332.35−0.43	16 17 31.6	−51 08 21	−53.1[27]	5.5	11.4	3.7	5.5	11.3	3.6	8
332.55−0.14	16 17 12.09	−50 47 12.0	−46.7[3]	5.7	11.7	3.4	5.7	11.7	3.2	5,8,43,44
332.60−0.16	16 17 29.19	−50 46 11.6	−50.9[27]	5.6	11.5	3.6	5.6	11.5	3.5	5,8
332.65−0.62	16 19 43.48	−51 03 36.5	−49.5[14]	5.6	11.6	3.5	5.6	11.5	3.4	4,43,44
332.72−0.62	16 20 01.3	−51 00 44	−46.0[27]	5.8	11.8	3.3	5.7	11.7	3.2	4
332.94−0.68	16 21 19.0	−50 54 10	−52.9[27]	5.5	11.4	3.7	5.5	11.4	3.6	8
332.96+0.77	16 15 01.06	−49 50 40.0	−44.5[3]	5.8	11.9	3.2	5.8	11.8	3.1	43
332.96−0.67	16 21 22.9	−50 52 58	−45.9[27]	5.7	11.8	3.3	5.7	11.7	3.2	8
333.02−0.01	16 18 44.06	−50 21 51.7	−55.2[27]	5.4	11.3	3.8	5.4	11.3	3.7	5,8
333.02−0.06	16 18 56.71	−50 23 55.1	−53.6[27]	5.4	11.4	3.7	5.4	11.4	3.6	8,5
333.06−0.44	16 20 50.3	−50 38 43	−59.0[42]	5.2	11.1	4.0	5.3	11.1	3.9	4,8
333.12−0.43	16 20 59.71	−50 35 52.0	−52.0[14]	5.5	11.5	3.7	5.5	11.5	3.5	17,4,8,43,44
333.12−0.56	16 21 35.4	−50 40 57	−56.8[27]	5.3	11.3	3.9	5.3	11.2	3.8	8
333.16−0.10	16 19 42.68	−50 19 54.5	−91.8[3]	4.3	9.5	5.6	4.4	9.7	5.3	4,5,8,43
333.18−0.09	16 19 45.67	−50 18 35.5	−91.8[3]	4.3	9.6	5.6	4.4	9.7	5.3	4,5,8
333.23−0.06	16 19 51.39	−50 15 15.0	−92.0[42]	4.3	9.5	5.6	4.4	9.7	5.3	4,5,8
333.31+0.10	16 19 29.09	−50 04 42.0	−45.0[27]	5.8	11.9	3.3	5.7	11.8	3.2	5,8
333.46−0.16	16 21 20.17	−50 09 49.0	−45.3[3]	5.7	11.9	3.3	5.7	11.8	3.2	17,4,5,8,43,44
333.56−0.02	16 21 08.86	−49 59 49.0	−35.8[27]	6.2	12.5	2.8	6.1	12.3	2.7	5,8
333.64+0.05	16 21 09.23	−49 52 44.2	−87.3[27]	4.4	9.8	5.4	4.4	9.9	5.1	5,8
333.68−0.43	16 23 29.8	−50 12 08	−5.2[27]	8.1	14.7	0.5	7.8	14.4	0.7	8
333.93−0.13	16 23 15.00	−49 48 48.7	−36.7[27]	6.1	12.4	2.8	6.0	12.3	2.8	5,8
334.63−0.01	16 25 45.78	−49 13 38.2	−30.0[27]	6.4	12.9	2.4	6.3	12.8	2.4	5,8
334.93−0.09	16 27 24.26	−49 04 10.6	−19.5[27]	7.0	13.7	1.7	6.9	13.5	1.8	5,8
335.06−0.42	16 29 23.1	−49 12 27	−47.0[27]	5.6	12.0	3.5	5.6	11.9	3.3	8
335.55−0.31	16 30 55.3	−48 46 14	−116.0[27]	3.6	8.6	6.9	3.7	8.9	6.4	4
335.58−0.29	16 30 58.79	−48 43 53.0	−46.6[3]	5.5	12.0	3.5	5.5	12.0	3.3	17,4,5,44
335.60−0.07	16 30 07.20	−48 34 22.1	−50.4[27]	5.4	11.8	3.7	5.4	11.8	3.5	5
335.72+0.19	16 29 27.25	−48 17 54.3	−44.3[27]	5.6	12.2	3.3	5.6	12.1	3.2	5
335.78+0.17	16 29 47.34	−48 15 52.0	−47.5[27]	5.5	12.0	3.5	5.5	11.9	3.4	4,5
336.01−0.82	16 35 09.3	−48 46 47	−48.3[3]	5.4	12.0	3.6	5.4	11.9	3.5	39,43,44
336.35−0.13	16 33 29.15	−48 03 44.0	−79.6[3]	4.4	10.5	5.1	4.4	10.6	4.8	17,4,5,43,44
336.41−0.26	16 34 14.1	−48 06 26	−92.0[42]	4.0	10.0	5.6	4.1	10.1	5.3	4
336.43−0.26	16 34 19.0	−48 05 33	−92.0[42]	4.0	10.0	5.6	4.1	10.1	5.3	4,43
336.82+0.02	16 34 38.18	−47 36 33.3	−76.7[27]	4.4	10.7	5.0	4.5	10.7	4.7	17,4,5
336.83−0.38	16 36 26.4	−47 52 28	−22.3[3]	6.7	13.6	2.0	6.6	13.4	2.0	39
336.86+0.00	16 34 54.43	−47 35 37.5	−73.3[3]	4.5	10.8	4.8	4.5	10.9	4.6	4,5,43,44
336.94−0.15	16 35 55.13	−47 38 44.7	−67.3[27]	4.7	11.1	4.5	4.7	11.1	4.4	5

Table 5. continued.

Source name	RA(2000) (^{h} ^{m} ^{s})	Dec(2000) ($^\circ$ $'$ $''$)	V_{LSR} (km s^{-1})	Θ_0 = 220 km s^{-1} R (kpc)	d_{far} (kpc)	d_{near} (kpc)	Θ_0 = 254 km s^{-1} R (kpc)	d_{far} (kpc)	d_{near} (kpc)	Ref.
336.98−0.18	16 36 12.31	−47 37 58.4	−80.8[27]	4.3	10.5	5.1	4.3	10.6	4.9	5
336.99−0.02	16 35 33.98	−47 31 11.5	−120.9[3]	3.4	8.6	7.0	3.5	9.0	6.5	4,5,43,44
337.09−0.21	16 36 46.36	−47 34 24.1	0.0[27]	8.5	15.7	0.1	8.2	15.3	0.2	44
337.15−0.40	16 37 50.9	−47 39 09	−49.4[9]	5.3	12.0	3.7	5.3	11.9	3.6	9
337.17−0.03	16 36 18.78	−47 23 18.6	−65.6[3]	4.7	11.2	4.5	4.7	11.2	4.3	5
337.25−0.10	16 36 56.43	−47 22 27.0	−69.3[27]	4.6	11.0	4.6	4.6	11.0	4.4	5
337.39−0.20	16 37 55.9	−47 20 58	−56.4[9]	5.0	11.6	4.1	5.0	11.6	3.9	9
337.40−0.40	16 38 50.51	−47 28 00.5	−41.3[14]	5.6	12.4	3.3	5.6	12.3	3.2	17,4,43,44
337.61−0.05	16 38 09.53	−47 05 00.0	−49.7[3]	5.2	12.0	3.7	5.3	11.9	3.6	4,5,43,44
337.68+0.13	16 37 35.41	−46 53 49.5	−74.9[27]	4.4	10.8	4.9	4.4	10.9	4.7	5
337.70−0.05	16 38 29.62	−47 00 35.0	−48.1[3]	5.3	12.1	3.7	5.3	12.0	3.5	5,43,44
337.71+0.08	16 37 53.58	−46 54 41.0	−72.6[27]	4.4	10.9	4.8	4.5	10.9	4.6	5
337.92−0.46	16 41 06.05	−47 07 02.0	−38.7[14]	5.7	12.6	3.1	5.7	12.5	3.1	17,4,43,44
337.96−0.16	16 40 01.07	−46 53 33.2	−60.4[27]	4.8	11.5	4.3	4.8	11.5	4.1	5,51
338.00+0.13	16 38 50.8	−46 40 05	−32.0[27]	6.0	13.0	2.7	6.0	12.9	2.7	4
338.07+0.01	16 39 39.04	−46 41 28.0	−40.5[3]	5.6	12.5	3.3	5.6	12.4	3.2	17,5,44
338.28+0.54	16 38 09.6	−46 11 09	−57.0[27]	4.9	11.7	4.1	4.9	11.6	4.0	4
338.28+0.12	16 40 00.07	−46 27 38.3	−39.3[27]	5.6	12.6	3.2	5.6	12.5	3.1	5
338.43+0.05	16 40 49.81	−46 23 36.5	−32.3[3]	6.0	13.0	2.8	6.0	12.9	2.7	39,5,43,44
338.46−0.24	16 42 15.48	−46 34 18.5	−50.4[27]	5.1	12.0	3.8	5.2	11.9	3.7	17,4,5,43,44
338.47+0.29	16 39 58.1	−46 12 39	−30.0[27]	6.1	13.2	2.6	6.1	13.0	2.6	13,4
338.56+0.11	16 41 06.98	−46 15 30.1	−75.0[27]	4.3	10.9	5.0	4.4	10.9	4.7	5
338.87−0.08	16 43 08.21	−46 09 13.9	−41.4[27]	5.5	12.5	3.4	5.5	12.4	3.2	17,4,5
338.92+0.55	16 40 34.1	−45 42 06	−66.0[42]	4.5	11.3	4.6	4.6	11.3	4.4	17,4
338.92+0.38	16 41 17.71	−45 48 21.0	−26.0[27]	6.3	13.5	2.4	6.3	13.3	2.4	43
338.93−0.06	16 43 16.1	−46 05 39	−41.9[27]	5.5	12.5	3.4	5.5	12.4	3.3	4,5
339.05−0.31	16 44 49.09	−46 10 14.0	−111.6[27]	3.4	9.5	6.4	3.5	9.6	6.1	5
339.06+0.15	16 42 49.65	−45 51 22.7	−85.6[27]	4.0	10.5	5.4	4.0	10.5	5.2	5
339.28+0.13	16 43 43.05	−45 42 08.5	−69.1[27]	4.4	11.2	4.7	4.5	11.2	4.5	5
339.29+0.13	16 43 44.97	−45 41 28.8	−74.6[27]	4.2	10.9	5.0	4.3	11.0	4.8	5
339.47+0.04	16 44 51.00	−45 36 56.4	−9.3[27]	7.6	14.9	1.0	7.4	14.6	1.1	5
339.58−0.12	16 45 58.84	−45 38 47.0	−33.2[3]	5.9	13.0	2.9	5.8	12.9	2.8	5,44
339.62−0.12	16 46 05.98	−45 36 43.5	−33.2[3]	5.9	13.0	2.9	5.8	12.9	2.8	17,4,5,43,44
339.68−1.21	16 51 06.21	−46 16 03.0	−21.0[27]	6.6	13.9	2.1	6.5	13.7	2.1	17,4,43,44
339.76+0.05	16 45 51.72	−45 23 32.2	−51.0[27]	5.0	12.0	3.9	5.0	12.0	3.8	5
339.88−1.25	16 52 04.67	−46 08 34.0	−31.6[3]	5.9	13.1	2.8	5.9	13.0	2.8	4,43,44
339.94−0.53	16 49 08.00	−45 37 58.5	−89.0[31]	3.8	10.4	5.6	3.9	10.5	5.3	43,44
340.03−0.29	16 48 21.44	−45 24 33.5	−60.0[27]	4.6	11.6	4.4	4.7	11.6	4.2	17,4,43,44
340.25−0.05	16 48 07.37	−45 05 10.0	−121.9[3]	3.1	9.2	6.8	3.2	9.4	6.4	43
340.53−0.15	16 49 33.7	−44 56 03	−48.3[51]	5.0	12.2	3.9	5.1	12.1	3.7	51
340.79−0.10	16 50 17.0	−44 42 22	−107.0[27]	3.3	9.8	6.2	3.4	9.9	6.0	4
340.97−1.03	16 54 58.7	−45 09 23	−31.4[9]	5.8	13.2	2.9	5.8	13.1	2.8	9
341.22−0.21	16 52 17.9	−44 26 41	−43.4[3]	5.2	12.4	3.7	5.2	12.4	3.5	4
341.28+0.06	16 51 20.8	−44 13 36	−74.0[27]	4.0	11.0	5.1	4.1	11.1	4.9	13,4
342.36+0.14	16 54 49.14	−43 20 03.0	−6.0[27]	7.8	15.4	0.8	7.6	15.1	0.9	43,44
342.50+0.17	16 55 07.2	−43 12 54	−41.8[51]	5.1	12.5	3.7	5.1	12.5	3.5	51
343.52−0.50	17 01 27.7	−42 49 44	−33.9[3]	5.4	13.0	3.3	5.4	12.9	3.2	9
343.92+0.12	17 00 10.90	−42 07 19.5	14.0[27]	11.1	19.1		10.4	18.2		17,4,43,44
344.22−0.56	17 04 07.7	−42 18 39	−23.2[3]	6.0	13.8	2.6	6.0	13.6	2.5	18,4,43,44
344.42+0.04	17 02 08.76	−41 46 58.0	−65.9[3]	3.9	11.4	5.0	4.0	11.4	4.8	18,4,43,44
344.58−0.02	17 02 57.73	−41 41 54.0	−1.0[3]	8.4	16.2	0.2	8.1	15.8	0.4	20,4,43,44
345.00−0.22	17 05 10.90	−41 29 06.5	−26.2[14]	5.7	13.5	2.9	5.7	13.4	2.8	20,4,43,44
345.01+1.79	16 56 47.56	−40 14 25.5	−13.4[14]	6.8	14.7	1.8	6.7	14.5	1.8	20,4,43,44
345.20−0.04	17 05 01.0	−41 13 09	−0.7[9]	8.4	16.3	0.1	8.1	15.9	0.3	9
345.42−0.95	17 09 38.57	−41 35 04.0	−21.2[14]	6.1	13.9	2.5	6.0	13.8	2.5	4,43,44
345.50+0.34	17 04 22.89	−40 44 23.0	−16.3[14]	6.5	14.4	2.1	6.4	14.2	2.1	20,4,43,44
345.69−0.09	17 06 51.3	−40 50 59	0.0[27]	8.5	16.5	0.1	8.2	16.1	0.2	20
345.83+0.04	17 06 42.28	−40 39 26.0	−10.0[31]	7.1	15.1	1.4	7.0	14.8	1.5	43,44
346.42+0.28	17 07 33.7	−40 03 04	−18.7[51]	6.2	14.1	2.4	6.1	13.9	2.4	51
346.48+0.13	17 08 23.1	−40 05 33	3.0[31]	9.0	17.1		8.7	16.6		13,4
346.52+0.08	17 08 43.1	−40 05 25	3.0[31]	9.0	17.1		8.7	16.6		4,43

Table 5. continued.

Source name	RA(2000) (h m s)	Dec(2000) (° ′ ″)	V_{LSR} (km s^{-1})	Θ_0 = 220 km s^{-1} R (kpc)	d_{far} (kpc)	d_{near} (kpc)	Θ_0 = 254 km s^{-1} R (kpc)	d_{far} (kpc)	d_{near} (kpc)	Ref.
347.58+0.21	17 11 26.8	−39 09 37	−103.0[27]	2.6	10.1	6.5	2.7	10.1	6.3	4,43
347.63+0.21	17 11 36.14	−39 07 06.5	−97.0[27]	2.7	10.2	6.4	2.8	10.3	6.1	17,4,44
347.82+0.02	17 12 58.0	−39 04 43	−25.0[27]	5.4	13.4	3.2	5.4	13.3	3.1	4
347.86+0.01	17 13 06.22	−39 02 40.5	−30.0[31]	5.1	13.0	3.6	5.1	13.0	3.5	17,4,44
347.90+0.05	17 13 05.1	−38 59 46	−30.0[31]	5.1	13.0	3.6	5.1	13.0	3.5	4,43
348.23−0.97	17 18 23.88	−39 19 10.0	−13.7[3]	6.4	14.5	2.1	6.4	14.3	2.1	43
348.55−0.98	17 19 20.8	−39 03 53	−15.7[14]	6.2	14.3	2.4	6.1	14.1	2.4	13,4,43
348.70−1.04	17 20 04.02	−38 58 30.0	−12.3[14]	6.6	14.7	2.0	6.4	14.5	2.0	20,4,43,44
348.88+0.10	17 15 48.4	−38 10 18	−75.0[27]	3.0	10.8	5.9	3.0	10.8	5.7	13,4
348.89−0.18	17 17 00.24	−38 19 29.5	7.9[3]	10.5	18.7		9.9	18.0		4,43,44
349.07−0.02	17 16 51.9	−38 05 12	7.0[27]	10.3	18.5		9.7	17.8		4
349.09+0.10	17 16 24.72	−37 59 47.0	−77.0[27]	2.9	10.7	6.0	3.0	10.7	5.8	17,4,43,44
350.01+0.43	17 17 45.47	−37 03 12.0	−31.5[3]	4.6	12.7	4.1	4.6	12.6	3.9	13,4,43,44
350.10+0.08	17 19 27.03	−37 10 53.5	−69.5[3]	2.9	10.9	5.9	3.0	10.9	5.7	20,4,43,44
350.29+0.12	17 19 50.86	−37 00 00.5	−64.0[27]	3.0	11.0	5.7	3.1	11.0	5.5	32,43,44
350.69−0.50	17 23 31.6	−37 01 40	−18.6[3]	5.5	13.7	3.1	5.5	13.6	3.0	39
351.16+0.69	17 19 58.84	−35 57 40.5	−6.1[14]	7.2	15.4	1.4	7.0	15.2	1.4	20,4,43,44
351.23+0.66	17 20 17.8	−35 54 58	−3.5[30]	7.7	16.0	0.8	7.4	15.6	1.0	20
351.41+0.64	17 20 53.37	−35 47 02.0	−6.9[3]	7.0	15.3	1.5	6.8	15.0	1.6	20,4,43,44
351.58−0.35	17 25 25.19	−36 12 45.5	−98.5[3]	2.0	10.0	6.9	2.1	10.0	6.6	17,4,43,44
351.77−0.53	17 26 42.56	−36 09 17.5	−3.4[3]	7.6	16.0	0.9	7.4	15.6	1.0	20,4,43,44
352.08+0.16	17 24 42.4	−35 30 42	−67.0[27]	2.5	10.7	6.2	2.6	10.7	6.0	4
352.11−0.17	17 26 08.0	−35 40 19	−55.0[27]	2.9	11.1	5.8	3.0	11.1	5.6	4
352.12−0.93	17 29 17.6	−36 04 41	−12.0[27]	6.0	14.3	2.5	5.9	14.1	2.5	39
352.52−0.16	17 27 13.0	−35 19 34	−49.2[3]	3.0	11.2	5.6	3.1	11.2	5.4	13,4,43
352.60−0.18	17 27 32.04	−35 16 15.0	−86.5[3]	2.0	10.1	6.8	2.1	10.1	6.6	43
352.63−1.06	17 31 13.88	−35 44 08.0	−0.4[3]	8.4	16.7	0.1	8.0	16.3	0.4	32,43,44
353.21−0.23	17 29 25.45	−34 47 27.0	−17.3[3]	5.0	13.3	3.5	5.0	13.3	3.4	43
353.40−0.36	17 30 26.18	−34 41 45.0	−16.7[3]	5.0	13.4	3.5	5.0	13.3	3.4	20,4,43,44
353.46+0.56	17 26 51.5	−34 08 40	−47.1[3]	2.8	11.1	5.8	2.9	11.1	5.6	17,4,43
354.61+0.47	17 30 16.8	−33 14 13	−21.0[3]	4.1	12.5	4.4	4.1	12.4	4.3	20,4,43
354.72+0.30	17 31 15.55	−33 14 06.0	93.0[27]	25.0	33.5		25.0	33.4		32,43,44
355.34+0.14	17 33 28.92	−32 47 49.0	14.6[3]	25.0	33.5		25.0	33.4		20,4,43,44
356.66−0.27	17 38 30.5	−31 54 57	−52.3[3]	1.6	10.0	7.0	1.6	10.0	6.8	13,4,43
357.96−0.17	17 41 20.2	−30 45 47	−5.1[3]	5.1	13.5	3.4	5.0	13.4	3.4	39
358.27−2.08	17 49 41.6	−31 29 30	5.2[27]	25.0	33.5		25.0	33.4		39,33
358.37−0.46	17 43 31.95	−30 34 11.0	−3.0[3]	5.7	14.2	2.8	5.5	13.9	2.9	32,43,44
359.13+0.03	17 43 25.67	−29 39 17.5	−4.0[27]	3.7	12.2	4.8	3.7	12.1	4.7	20,4,6,43,44
359.43−0.10	17 44 40.66	−29 28 17.6	−52.0[27]	0.3	8.8	8.2	0.3	8.7	8.1	20,4,6
359.61−0.24	17 45 39.08	−29 23 29.0	22.5[27]	25.0	33.5		25.0	33.4		20,4,6
359.89−0.06	17 45 38.2	−29 03 28	10.0[27]	25.0	33.5		25.0	33.4		20
359.97−0.45	17 47 20.15	−29 11 57.2	19.1[14]	25.0	33.5		25.0	33.4		20,4,6,43

The first column lists the source name. The next two columns give their J2000 equatorial coordinates. Column (4) shows the radial velocity of peak emission from molecular lines, such as CS, CO and NH_3, etc., if available, otherwise from the maser peak. Columns (5)–(7) present the Galactic center distance, far and near kinematic distances calculated using the Galactic rotation model of Wouterloot & Brand (1989), assuming R_0 = 8.5 kpc and Θ_0 = 220 km s^{-1}. Columns (8)–(10) are the same as Columns (5)–(7), but revised using new R_0 and Θ_0 from Reid et al. (2009).
References:
1 – Anglada et al. (1996). 2 – Beuther & Sridharan (2007). 3 – Bronfman et al. (1996). 4 – Caswell et al. (1995a). 5 – Caswell (1996a). 6 – Caswell (1996b). 7 – Churchwell et al. (1990). 8 – Ellingsen et al. (1996). 9 – Ellingsen (2007). 10 – Felli et al. (1992). 11 – Fontani et al. (2006). 12 – Garay et al. (1993). 13 – Gaylard & Macleod (1993). 14 – Juvela (1996). 15 – Kim & Koo (2003). 16 – Larionov et al. (1999). 17 – Macleod & Gaylard (1992). 18 – Macleod et al. (1993). 19 – Mauersberger et al. (1986). 20 – Menten (1991). 21 – Minier et al. (1998). 22 – Minier et al. (2000). 23 – Minier et al. (2001). 24 – Minier et al. (2003). 25 – Molinari et al. (1996). 26 – Pandian et al. (2007). 27 – Pestalozzi et al. (2005). 28 – Pillai et al. (2006); 29 – Pirogov et al. (2006). 30 – Plume et al. (1992). 31 – Russeil (2003). 32 – Schutte et al. (1993). 33 – Slysh et al. (1999). 34 – Solomon et al. (1987). 35 – Szymczak et al. (2000). 36 – Szymczak et al. (2002). 37 – Szymczak et al. (2007). 38 – Teyssier et al. (2002). 39 – van der Walt et al. (1995). 40 – van der Walt et al. (1996). 41 – van der Walt et al. (2007). 42 – Vilas-Boas et al. (2000). 43 – Walsh et al. (1997). 44 – Walsh et al. (1998). 45 – Wouterloot & Brand (1989). 46 – Wouterloot et al. (1993). 47 – Wu et al. (2006). 48 – Xu et al. (2008). 49 – Zhang et al. (2005). 50 – Zinchenko et al. (1995). 51 – MacLeod et al. (1998). 52 – this paper.